Geographic information systems applied to rock slope stability analysis in Yellowstone County, Montana
by Edwin Jay DeYoung

A thesis submitted in partial fulfillment of the requirements for the degree of Master of Science in Earth Sciences
Montana State University

Abstract:
There are over 200 mapped slope failures in Yellowstone County, Montana. This study uses Geographic Information Systems (GIS) analysis to predict slope-failure hazard. Most regional slope stability analyses do not address discontinuity factors although such discontinuities are widely recognized as important. This analysis tests the importance of bedding-plane discontinuities in Yellowstone County.

Data layers consist of ARC/INFO grids with values of slope gradient, material type, slope type and the distance to the nearest lithologic contact for each 30 meter cell of the study area. Average slope gradient was calculated from U.S. Geologic Survey 30m Digital Elevation Models. Material type was categorized as the dominate lithologic material (sandstone, shale or mixed) in each cell area. A surface was created from near surface structure to represent bedding layers parallel to lithologic units. Slope type was determined from the relative structure gradient (dip) and slope gradient, identifying key areas having similar structure orientation and slope aspect. A stepwise discriminant analysis was used to determine the combination of slope, material, slope type and contact distance factors to determine the combination of variables to maximize the difference between mapped landslide locations and a set of stable slope cells.

Slope gradient is the strongest discriminating factor, and accounts for nearly 80% of the variance in the discriminant function. Material type has minimal significance and slope type is insignificant in discriminating between failed and stable slopes in this study. The distance to contacts with relatively hard lithologic units overlying relatively soft lithologic units is significant in discriminating between failed and stable slopes, accounting for nearly 20% of the discriminant variance. The origin of these relationships is probably related to mass movement.

Bedding discontinuity is a relevant factor although bedding is not a significant factor as determined for this study area. Overdip slope types are likely misclassified because the cell size (±250 m) approaches the size of mass-movement features. Site analysis shows discontinuities are a part of overall instability analysis, however, further work is needed to successfully incorporate bedding discontinuities in a regional stability analysis.

The probability of rock slope failure was determined for southern Yellowstone County, Montana from slope gradient, material type and the distance to the nearest hard over soft contact. This study does not give any site-specific information because input data was averaged to 30m grid cells and the resolution of combined analysis of multiple data sources is ~250m. The results indicate slope-failure probability for general areas. The maps can be used for regional assessment and emphasize where site-specific analysis is strongly recommended before development.

GEOGRAPHIC INFORMATION SYSTEMS APPLIED TO ROCK SLOPE STABILITY ANALYSIS IN YELLOWSTONE COUNTY, MONTANA

by

Edwin Jay DeYoung

A thesis submitted in partial fulfillment
of the requirements for the degree

of

Master of Science

in

Earth Sciences

MONTANA STATE UNIVERSITY - BOZEMAN
Bozeman, Montana

March 1996

N378
D5326

APPROVAL

of a thesis submitted by

Edwin Jay DeYoung

This thesis has been read by each member of the thesis committee and has been found to be satisfactory regarding content, English usage, format, citations, bibliographic style, and consistency, and is ready for submission to the College of Graduate Studies.

March 19 1996
Date

W Woch
Chairperson, Graduate Committee

Approved for the Major Department

March 19, 1996
Date

Dave [illegible]
Head, Major Department

Approved for the College of Graduate Studies

4/1/96
Date

[illegible]
Graduate Dean

STATEMENT OF PERMISSION TO USE

In presenting this thesis in partial fulfillment of the requirements for a master's degree at Montana State University - Bozeman, I agree that the Library shall make it available to borrowers under rules of the Library.

If I have indicated my intention to copyright this thesis by including a copyright notice page, copying is allowable only for scholarly purposes, consistent with "fair use" as prescribed in the U.S. Copyright Law. Requests for permission for extended quotation from or reproduction of this thesis in whole or in parts may be granted only by the copyright holder.

Signature Edwin Jay DeYoung

Date March 12, 1996

TABLE OF CONTENTS

TABLE OF CONTENTS - Continued

LIST OF TABLES

LIST OF FIGURES

LIST OF FIGURES - Continued

LIST OF FIGURES - Continued

Figure Page

ABSTRACT

There are over 200 mapped slope failures in Yellowstone County, Montana. This study uses Geographic Information Systems (GIS) analysis to predict slope-failure hazard. Most regional slope stability analyses do not address discontinuity factors although such discontinuities are widely recognized as important. This analysis tests the importance of bedding-plane discontinuities in Yellowstone County.

Data layers consist of ARC/INFO grids with values of slope gradient, material type, slope type and the distance to the nearest lithologic contact for each 30 meter cell of the study area. Average slope gradient was calculated from U.S. Geologic Survey 30m Digital Elevation Models. Material type was categorized as the dominate lithologic material (sandstone, shale or mixed) in each cell area. A surface was created from near surface structure to represent bedding layers parallel to lithologic units. Slope type was determined from the relative structure gradient (dip) and slope gradient, identifying key areas having similar structure orientation and slope aspect. A stepwise discriminant analysis was used to determine the combination of slope, material, slope type and contact distance factors to determine the combination of variables to maximize the difference between mapped landslide locations and a set of stable slope cells.

Slope gradient is the strongest discriminating factor, and accounts for nearly 80% of the variance in the discriminant function. Material type has minimal significance and slope type is insignificant in discriminating between failed and stable slopes in this study. The distance to contacts with relatively hard lithologic units overlying relatively soft lithologic units is significant in discriminating between failed and stable slopes, accounting for nearly 20% of the discriminant variance. The origin of these relationships is probably related to mass movement.

Bedding discontinuity is a relevant factor although bedding is not a significant factor as determined for this study area. Overdip slope types are likely misclassified because the cell size (±250 m) approaches the size of mass-movement features. Site analysis shows discontinuities are a part of overall instability analysis, however, further work is needed to successfully incorporate bedding discontinuities in a regional stability analysis.

The probability of rock slope failure was determined for southern Yellowstone County, Montana from slope gradient, material type and the distance to the nearest hard over soft contact. This study does <u>not</u> give any site-specific information because input data was averaged to 30m grid cells and the resolution of combined analysis of multiple data sources is ~250m. The results indicate slope-failure probability for general areas. The maps can be used for regional assessment and emphasize where site-specific analysis is strongly recommended before development.

CHAPTER 1

INTRODUCTION

Statement of Problem

Slope failure is a widespread natural hazard that poses a threat to life and property. Such failures are a problem in Yellowstone County, Montana (Yellowstone County Department of Planning, 1990). Assessment of where slopes are unstable is necessary for planning future development. Such planning would enhance opportunities to avoid building on unstable sites or encourage special design where building does occur in such cases (National Research Council, 1985). One approach to locating potentially unstable slopes is through analysis of slope instability factors through Geographic Information Systems (GIS) technology in Yellowstone County.

Figure 1.1 outlines the components addressed in this thesis on slope stability analysis. The pyramid structure represents stability prediction as the culminating goal. Identification of factors critical to slope stability is fundamental to the analysis. After the factors are identified, sources of information about the factors are collected. Collected data is imported into a GIS format. GIS is used to calculate derived layers which give additional information specific for slope stability analysis. Statistical analysis of data representing the determined factors allows prediction of potential slope instability for the study area.

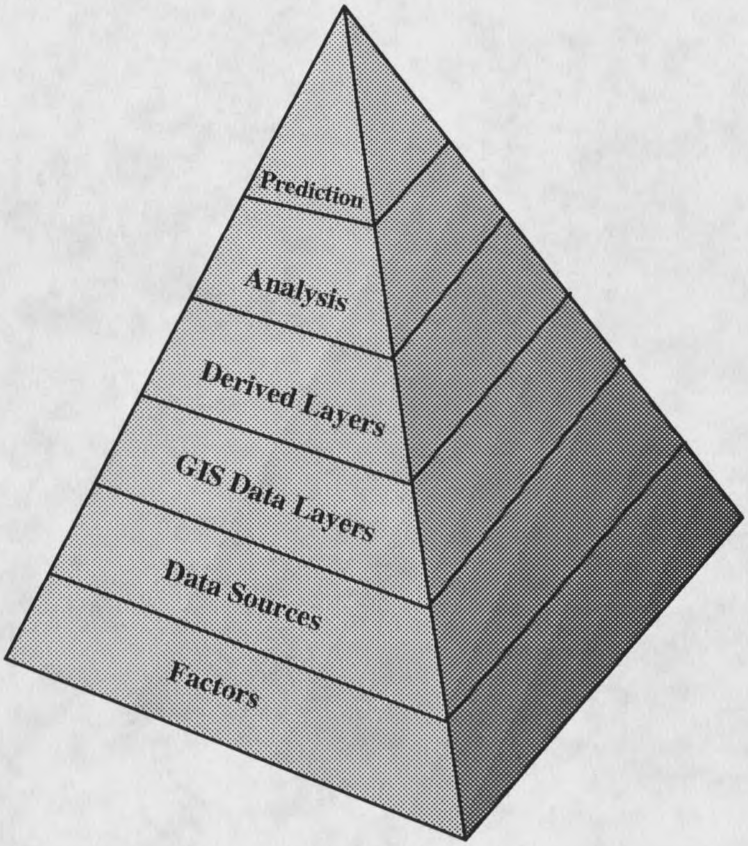

Figure 1.1. GIS model for prediction. Pyramid diagram shows order of model process from factor basis to final prediction.

GIS enables the processing of input data and the spatial analysis to evaluate locations of potential slope failure. Representation and analysis of multiple factors through space is feasible in GIS. Identification of appropriate land stability factors is fundamental for analysis and accurate predictions. Past GIS models have used factors of slope and material type but have generally left out geologic discontinuities. A model that incorporates such discontinuities is expected to better predict the location of unstable slopes than a model using slope and material alone. GIS technology enables rigorous instability analysis for large data sets for county sized regions, and is cost effective.

Study Area

The study area is the southern two-thirds of Yellowstone County, Montana (Fig. 1.2), where detailed elevation data are available. Billings, the most populous urban center of Montana, Laurel, several smaller towns and part of the Crow Indian Reservation are in the study area. The Yellowstone County Comprehensive Plan (Yellowstone County Planning Department, 1990) identifies slope stability as an important environmental geologic factor for planning and development. Three stated goals of the plan are to encourage designs which respect existing topographic features, take natural physical constraints into consideration, and promote safety in existing and new residential development. The aim of the county plan appears to be to inform residents of the existing natural hazards and to promote informed rational decisions about suitability for development.

This study will not provide the detailed information that is needed on a site-specific basis to make an informed decision about slope instability hazard. Rather, the intent of this study is to promote slope stability as a necessary consideration for development evaluation potential and indicate where site evaluations are critical for responsible development at a county-scale. More detailed site evaluations will be necessary because slope gradient, material type and all other slope characteristics vary at scales finer than 30 m x 30 m (the grid scale of the largest-scale GIS data layer).

Difference in topographic elevation is one of the bases for potential slope instability (Fig. 1.3). Overall relief in the area is 650 meters. The Pryor Mountains form a high area (1,518 m) at the southern edge of the study area. The lowest point (867 m) is in the northeast corner of the study area along the Yellowstone River. Elevation differences in Yellowstone

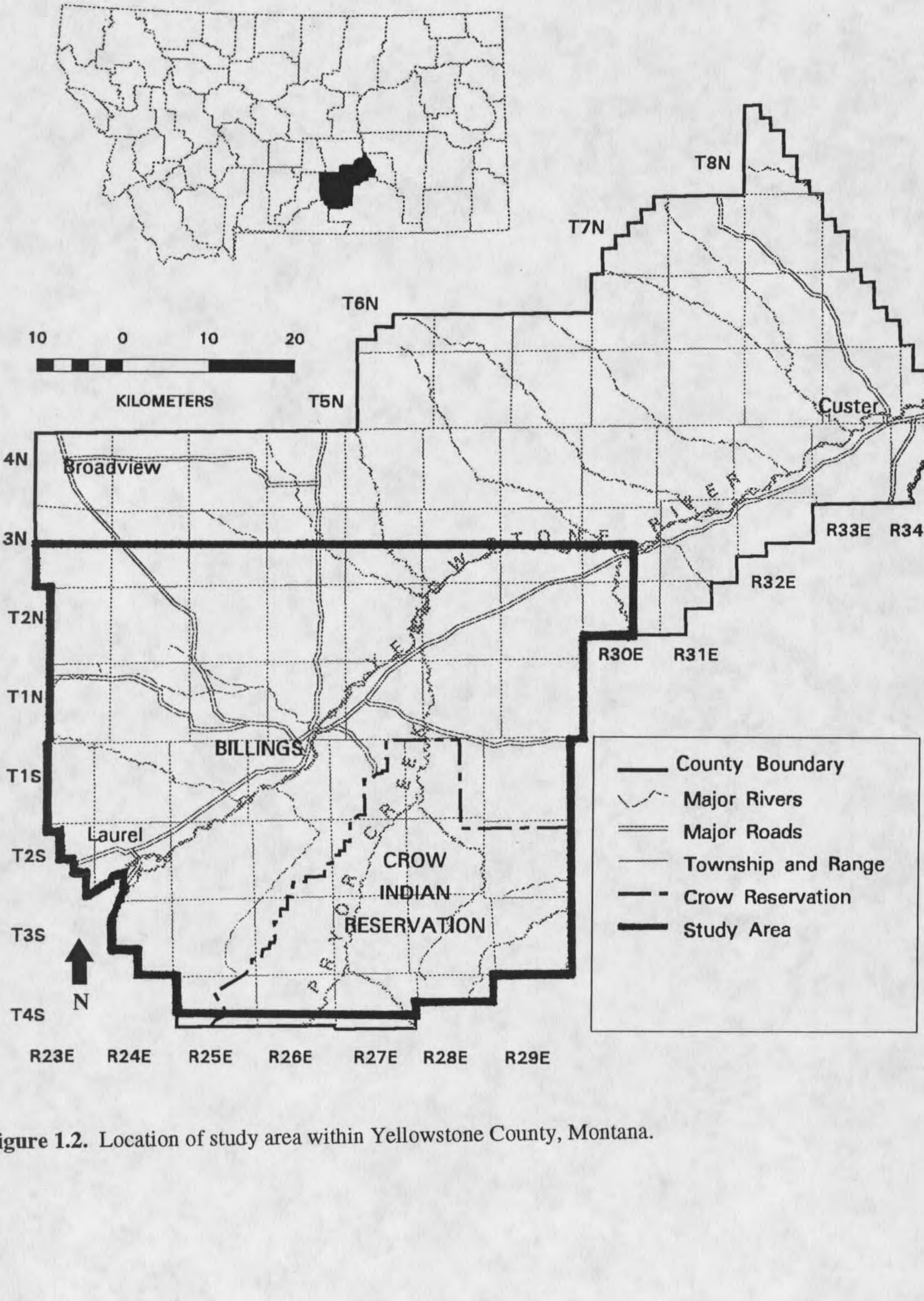

Figure 1.2. Location of study area within Yellowstone County, Montana.

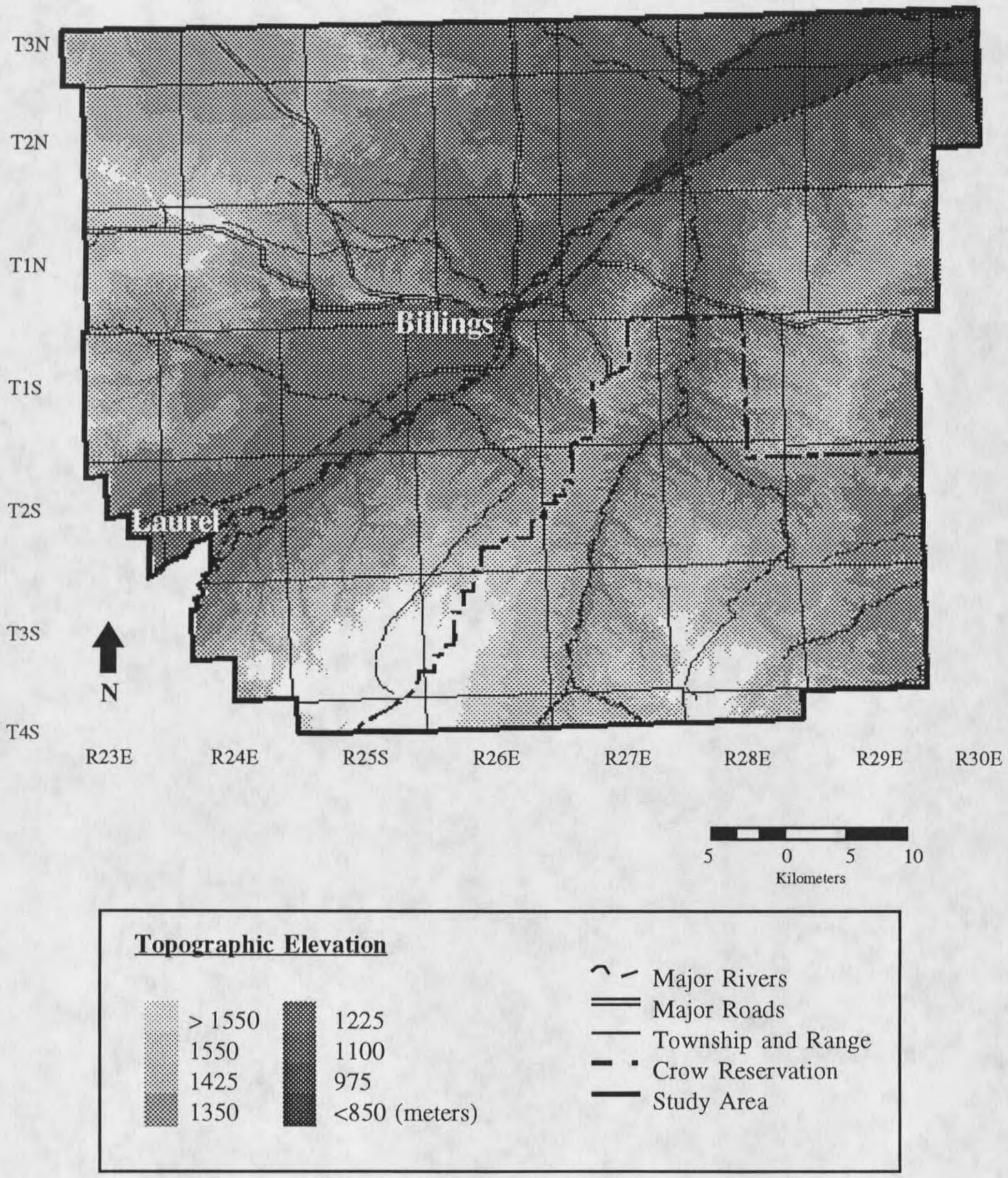

Figure 1.3. Topographic elevation.

County create potential for valley dissection, especially along Pryor Creek and its tributaries. Such tributary dissection forms steep slopes conducive to mass movement.

Topographic transitions from high to low areas are stepped due to alternating weak and strong Cretaceous shales and sandstones (Fig. 1.4). Resistant ridges and cliffs form in sandstones while gentle slopes and basins typify shales (Thom, 1935). The bedrock in the study area is Cretaceous in age. The Cloverly Formation, outcrops in a small area at the center of the southern edge of the study area (Fig.1.5). Moving up the stratigraphic column, the younger Cretaceous rocks of the Colorado Group outcrop north of the Cloverly in the southern part of the study area. The Montana group lies above the Colorado Group and outcrops to the north from near the southeast corner of the study area to the northern edge of the area. The Lance Formation, above the Montana Group, is the youngest Cretaceous formation in the study area and outcrops only in small areas along the northern edge of the study area. Tertiary gravel tops the butte rising above the Quaternary material in the southwest corner of Township 1 south, Range 24 east (Fig. 1.5). Quaternary sediments occur as fluvial deposits, terraces and fans along the Yellowstone River valley and as marsh sediments in the Comanche Basin near the northwest corner of the study area.

The geologic formations dip gently to the north off of the Pryor Mountain uplift at the southern margin of the study area. The dissected plains are formed on the layered Cretaceous sandstone and shales, which are stepped due to differing weathering rates and dissected by river tributaries. The Lake Basin and Fromberg fault zones locally complicate the geology (Fig.1.6). Topography reflects the combination of lithology and structure.

ERA	PERIOD		FORMATION	MEMBER		DESCRIPTION	CLASS
CENOZOIC	QUATERNARY				Qt	Gravel, Sand, Clay	
	TERTIARY				Tt	Gravel, Sand	
MESOZOIC	CRETACEOUS		Lance		Kl	Sandstone, Clay	Mix
		Montana Group	Lennep		Kle	Andesitic Sandstone	Ss
			Bearpaw		Kbp	Dark Marine Shale	Sh
			Judith River		Kjr	Interbedded Ss, Shale	Mix
			Claggett	Parkman	Kcp	Sandstone	Ss
					Kcg	Shale, Sandstones	Sh
			Eagle		Ke	Massive Sandstone	Ss
			Telegraph Creek		Kte	Sandy Shale, Sandstone	Mix
		Colorado Group	Niobrara - Carlile		Knc	Shale, Minor Sandy Beds	Sh
			Frontier	Torchlight	Kft	Sandstone	Ss
					Kf	Shale with thin Ss	Sh
			Mowrey		Km	Shale, Bentonite Zones	Sh
			Thermopolis		Kt	Shale Muddy Sandstone Shale	Sh
			Cloverly	Greybull	Kg	Sandstone	Ss
					Kcl	Volcanic Ash Chert Conglomerate, Ss	Sh
	JURASSIC		Morrison		Jm	Shale, Sandstone	

Figure 1.4. Stratigraphic column for south central Montana (From Knappen and Moulten, 1930, p.8-9). Symbol and description are given for every formation and prominent member in study area. Sandstone (Ss), shale (Sh) and mixed lithology (Mix) classifications shown are used in the analysis. The dashed line represents an unconformity, however, the Morrison outcrops just south of study area.

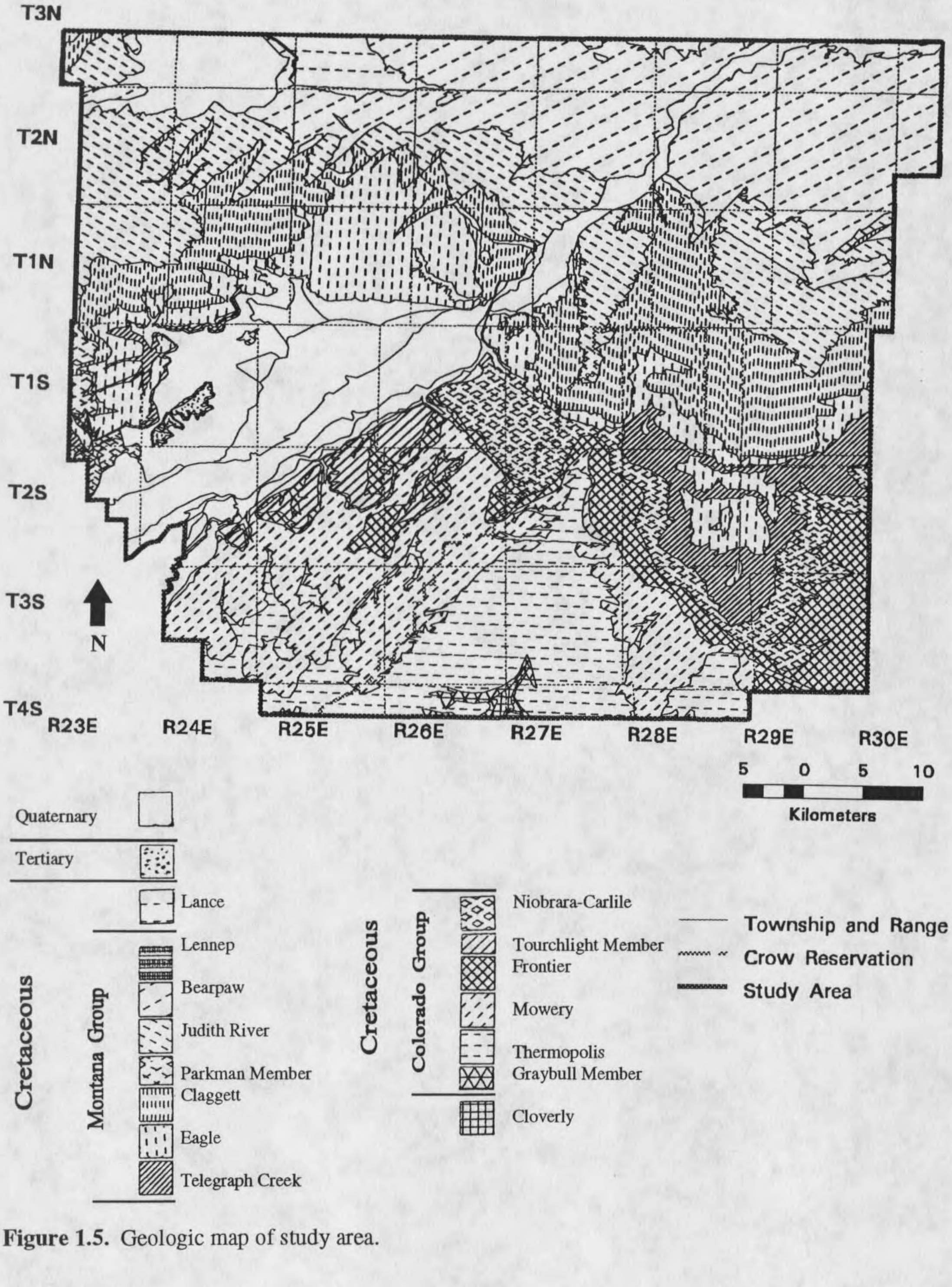

Figure 1.5. Geologic map of study area.

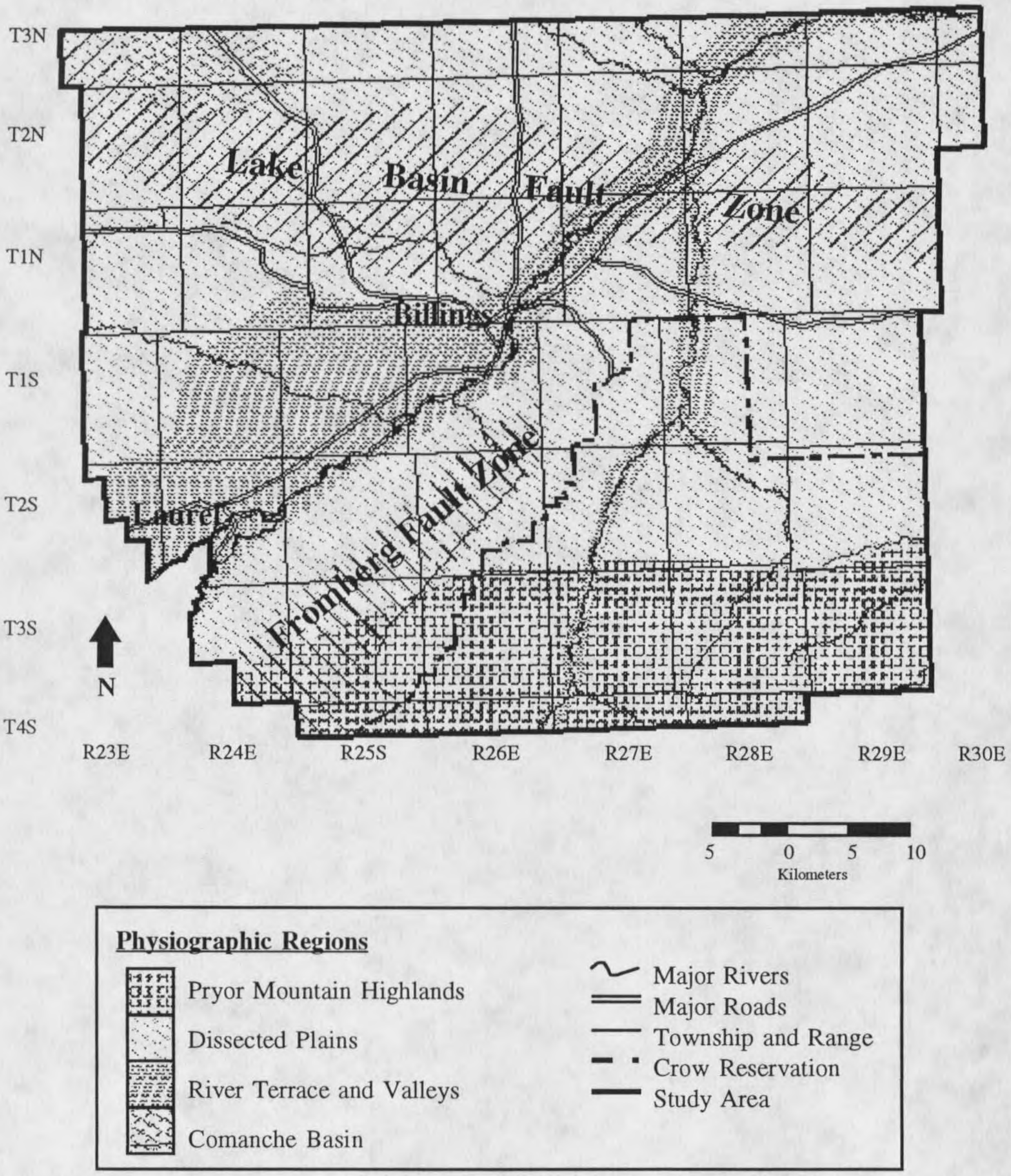

Figure 1.6. Physiographic regions and fault zones.

Slope instability hazard exists throughout the county because of the varying relief of the dissected topography on rocks of varying strength.

Review of Relevant Literature

The only published slope stability hazard analysis of Yellowstone County is included in a Montana Landslide Hazard Map (Fig. 1.7; Mills, 1987). Mills' (1987) map was produced using slope, geology and precipitation factors for cell areas of 21 km^2 (8 mi^2). Most of Yellowstone County has a moderate slope failure hazard according to Mills, but slope failure is locally recognized as an important consideration for development in the Yellowstone County Master Plan (Yellowstone County Department of Planning, 1990). A more detailed representation of the variability at the county scale is needed for slope stability analysis and planning in Yellowstone County.

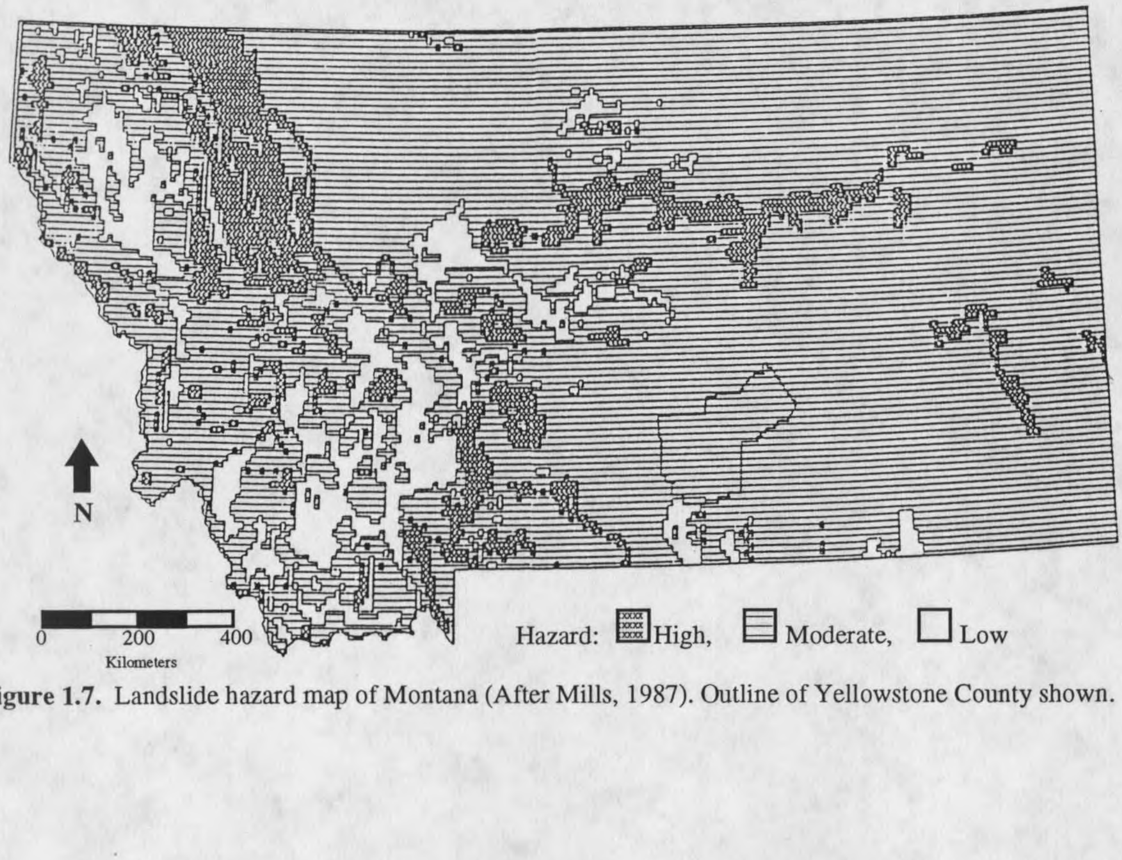

Figure 1.7. Landslide hazard map of Montana (After Mills, 1987). Outline of Yellowstone County shown.

One source of information on slope instability comes from a preliminary map of landslides in Montana (Wilde and others, unpublished, Fig. 1.8) which shows the location of 200 landslides in Yellowstone County. This map compiles the location of failures reported in the media and scientific literature. The data base associated with failure locations gives the source of the data but no failure type information. Small events of a few cubic meters, like the rockfalls along the Rimrocks (Eagle Sandstone) in Billings, are not included in the database even though they are known to occur.

Most small rock failures in the region are likely to be topples, but large failures are slides and, to a lesser extent, slumps. In incompetent rocks (like the Cretaceous section!) Both slumps and slides transition to flows downslope, regardless of water content. The hazard from slumps, slides and flows is similar in that all tend to be restricted to a fall/flow ratio of greater than 0.4, but the risk certainly varies from place to place depending on lithology and orientation of discontinuities.

Based on the map of landslide occurrence (Fig. 1.8), the slope stability hazard is not uniformly moderate. Past landslides are evidence of high future hazard. Large areas without mapped landslides may indicate little potential for hazard, but some such areas may have unmapped landslides or future mass movement potential. The characteristics of failed slopes may help in assessing the factors related to instability. A hazard map, which distinguishes failed areas and areas with similar characteristics from areas with no failures which have few characteristics in common with failed areas, provide a basis for proactive planning.

The stability of slopes depends on many factors (Table 1.1; Cooke and Doornkamp, 1990). These factors are grouped as intrinsic conditions of slope and extrinsic conditions

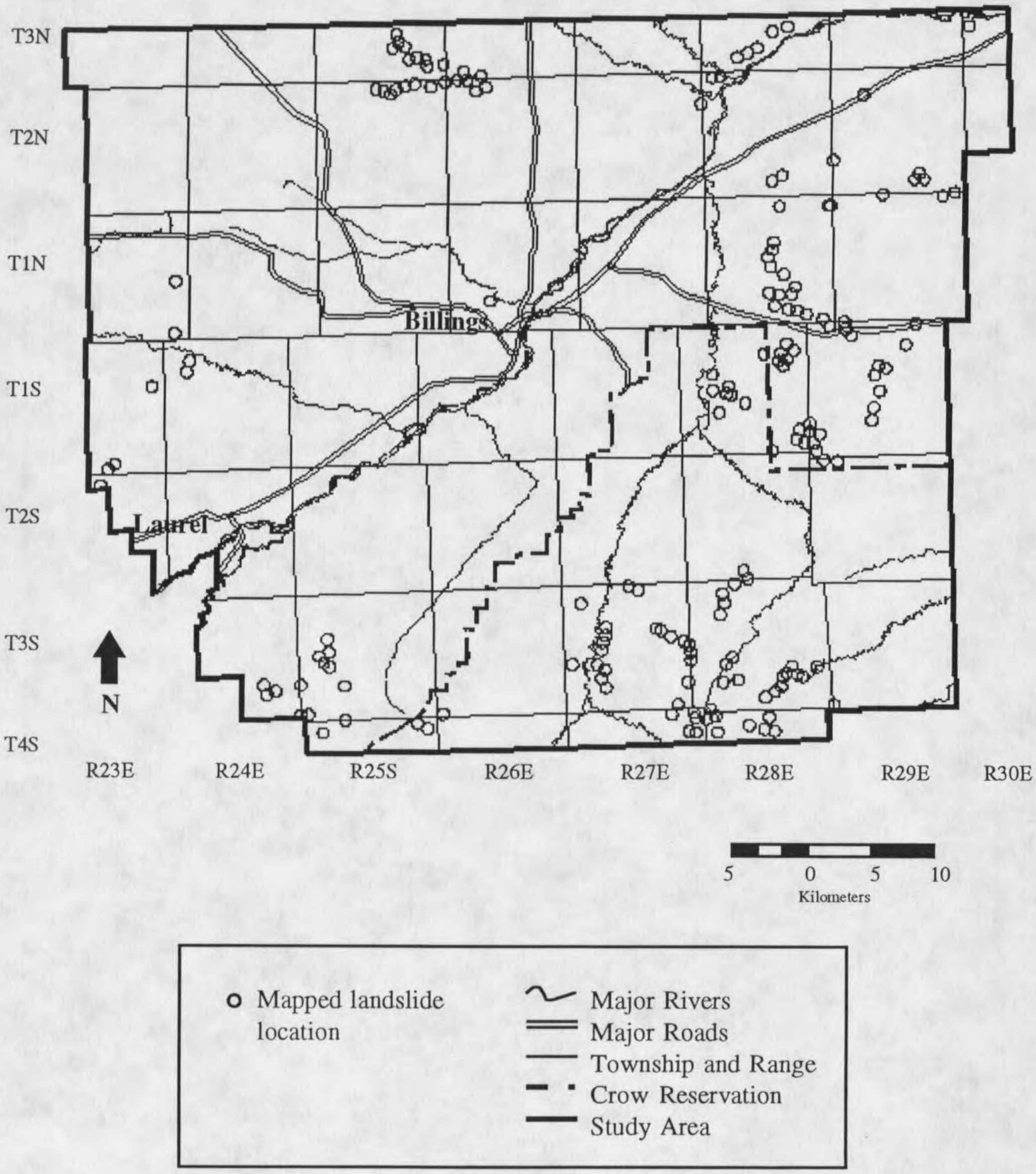

Figure 1.8. Location of mapped landslides in study area (From Wilde and others, unpublished).

acting on the slope. Extrinsic conditions are short term events which trigger slope failure. Intrinsic characteristics of topography, hydrology and material properties are long term 'causes' in slope stability. In order for a slope to fail, the intrinsic conditions have to be sufficiently weak for the extrinsic condition (a trigger event) to initiate failure. A planning map cannot predict *when* failure will occur, however, through analysis of internal conditions such a map can suggest *where* failure is likely.

Internal factors related to stability are largely related to the slope material. Cooke and Doornkamp (1990) separate material into bedrock and soil properties. Bedrock (a consolidated material) has very different physical properties than soil (an unconsolidated material). Each requires distinct characterizations. All of the mapped landslides in Yellowstone County are on Cretaceous rock units. Even though there is little distinction between the physical properties of weathered shale and soil, field analysis indicates that the depth of highly weathered shales is limited to less than ½ m on sloped areas. Because of the thin weathered depth the study is limited to an analysis of rock slope stability.

Accurate analysis of rock slope stability is a complex problem because of the many interacting factors. Factors include slope gradient, seismicity, vegetative cover, precipitation, and various hydrologic, topographic, and material properties (Table 1.2). External (triggering) and hydrologic properties have minimal representation in published slope stability studies. Typically, material properties of rock type or strength have been used. Discontinuities were recognized as important by Selby (1980) but have been ignored until recent work by Alexander and Formichi (1993).

TABLE 1.1. FACTORS RELATED TO LARGE-SCALE INSTABILITY
(After Cooke and Doornkamp, 1990, Table 5.5, p. 120-121).

	Earthquake	Tremor Frequency
	Human Activity	Excavation Location on Slope
		Excavation Depth
Short Term 'Triggers'		Lowering of Reservoir
		Reservoir
Extrinsic Conditions		Drainage Diversion
		Loading of Upper Valley Side
		Removal of Vegetation
	Climate	Rainstorm Event
		Snowmelt Event
	Topography	Valley Depth
		Slope Gradient
		Cliffs
		Valley Height Differences
	Hydrology	Drainage Density
		River Gradient
		Slope Undercutting
		Concentrated Seepage Flow
		Standing Water
		Recent Incision
		Pore Water Pressure
Long Term 'Causes'	**Material Properties (Rock)**	Jointing Density
		Jointing Openings
Intrinsic Conditions		Joint Orientation
		Joint Dip Relative to Slope
		Joint Gouge
		Strong Beds Over Weak Beds
		Degree of Weathering
		Compressive Strength
		Coherence
	Material Properties (Soil)	Coherent Over Incoherent Beds
		Depth
		Shear Strength
		Plastic Limit
		Liquid Limit

TABLE 1.2. CHRONOLOGICAL EVOLUTION OF FACTORS USED TO MODEL ROCK SLOPE STABILITY. COMPARISON OF INTRINSIC AND EXTRINSIC FACTORS USED IN 13 REGIONAL SLOPE STABILITY MODELS.

			a	b	c	d	e	f	g	h	I	j	k	l	m
INTRINSIC	Topographic	Slope Aspect	✓	✓	✓	✓				✓	✓	✓	✓		
		Slope Gradient	✓	✓	✓	✓	✓	✓	✓	✓	✓	✓	✓	✓	✓
		Slope Shape						✓		✓	✓		✓	✓	
		Elevation						✓		✓			✓	✓	
	Hydrologic	Drainage Density		✓	✓										✓
		River Gradient		✓											
		Pore Pressure					✓		✓						
		Seepage Flow	✓	✓				✓							
	Material	Jointing Density	✓									✓			✓
		Jointing Openings	✓												
		Joint Orientation	✓						✓				✓		✓
		Joint Dip	✓						✓				✓		✓
		Joint Fill	✓												
		Strong Over Weak Beds													
		Degree of Weathering	✓						✓						
		Material Strength	✓				✓				✓				
		Material Type		✓	✓	✓	✓		✓	✓		✓	✓		✓
EXTRINSIC		Seismicity				✓		✓						✓	
		Precipitation					✓								
		Vegetation Cover				✓				✓			✓	✓	
		Previous Landslides		✓			✓			✓	✓		✓		✓
			a	b	c	d	e	f	g	h	I	j	k	l	m

a. Alexander and Formichi, 1993
b. Carrara et al., 1991
c. Gao and Lo, 1991
d. Gupta and Joshi, 1990
e. Jibson and Keefer, 1989
f. Bernknoff et al., 1988
g. Cruden and Eaton, 1987
h. Duncan, Ward, and Anderson, 1987
I. Wieczorek, Wilson, and Harp, 1985
j. Carrara, 1983
k. Lessing, Messina, and Fonner, 1983
l. Churchill, 1982
m. Selby, 1980

Hydrologic properties are sparsely represented in past stability models. Selby (1980) argued that the importance of hydrologic factors is overshadowed by other factors related to rock slope stability because the hydrologic factor which most directly interacts with slope (outflow of groundwater) is the least significant independent slope strength factor (Table 1.3). Hydrologic factors of slope stability are usually analyzed for site analysis. Because this study is regional in nature and hydrologic variables usually vary temporally, these factors are not included in this analysis.

All previous models used slope gradient and many also used slope aspect or other topographic factors. Slope gradient is invariably used because of its theoretical importance. Without a gradient, there would be no potential for movement. The downslope component of the force of gravity parallel to the surface partly determines the state of slope stability (Wadge, 1988). Occurrence of mass movement on various slope gradients indicate that other factors resist more or less successfully the force of gravity along a slope. Slope aspect is often significant, presumably because of the effect of aspect on evapotranspiration, and the water balance of the slope.

The mechanical properties of the slope material are also integral to stability. Discontinuities such as joints, faults, fractures and bedding planes are important to stability since they are locations where movement has occurred or will likely occur because of lower resistance than surrounding areas with out discontinuities. The nature of such discontinuities within the material (spacing, orientation, width, and continuity) is the most significant factor in rock slope stability (Table 1.3; Selby, 1980).

TABLE 1.3. ROCK MASS STRENGTH CLASSIFICATION. SLOPE STRENGTH r VALUES FOR 7 VARIABLES OF HIGH TO LOW SLOPE STRENGTHS WHERE SUM r < 26 IS RATED VERY WEAK, 50≤ SUM r > 26 IS RATED WEAK, 70 ≤ SUM > 50 IS RATED MODERATE, 90 ≤ SUM > 70 IS RATED STRONG, AND 100≤ SUM > 90 IS RATED VERY STRONG (AFTER SELBY, 1980, TABLE 6, p.44-45).

RELATIVE STRENGTH / VARIABLE	HIGH	MODERATELY HIGH	MODERATE	MODERATELY LOW	LOW
INTACT ROCK STRENGTH	>200 MPa r:20	100-200 MPa r:18	50-100 MPa r:14	25-50 MPa r:10	25-1 MPa r:5
WEATHERING	none r:10	slight r:9	moderate r:7	high r:5	complete r:3
SPACING OF DISCONTINUITY	> 3 m r:30	3-1 m r:28	1-0.3 m r:21	300-50 mm r:15	< 50 mm r:5
DISCONTINUITY ORIENTATION	steep dips into slope cross joints r:20	moderate dips into slope r:18	horizontal dips, or nearly vertical r:14	moderate dips out of slope r:9	steep dips out of slope r:8
WIDTH OF DISCONTINUITY	< 0.1 mm r:7	0.1 - 1 mm r:6	1 - 5 mm r:5	5 - 20 mm r:4	> 20 mm r:2
EXTENT OF DISCONTINUITY	none continuous r:7	few continuous r:6	continuous no infill r:5	continuous thin infill r:4	continuous thick infill r:1
OUTFLOW OF GROUNDWATER	none r:6	trace r:5	slight r:4	moderate r:3	great r:1

In sedimentary rocks bedding planes are the primary discontinuity. "The bedding planes are almost invariably surfaces of minimum shearing resistance" (Terzaghi, 1962, p.258). Slope aspect may be a good predictor because aspect accounts for discontinuity orientation. For example a southern aspect may correlate with failure when mechanism for failure is actually a bedding discontinuity orientation that dips to the south often at a lower angle than topographic slope. Bedding planes will be the type of discontinuity analyzed in this study.

The relative orientation of bedding planes with respect to the topographic aspect is an important slope stability factor (Cruden, 1988). Where the topographic aspect is in the same direction as the orientation of bedding dip (Fig. 1.9A), slopes are termed *cataclinal*; where the topographic aspect is in the opposite direction as bedding dip, slopes are termed *anaclinal*. Slopes where the topographic aspect and the orientation of bedding dip are not parallel are termed *plagioclinal*; except for *orthoclinal* slopes, where the topographic aspect is nearly perpendicular to the orientation of bedding dip. Cataclinal slopes (Fig. 1.9B) are further subdivided into underdip slopes (where the surface gradient is less than the dip of bedding), and overdip slopes (where the gradient is equal to or greater than dip) (Briggs et. al., 1975).

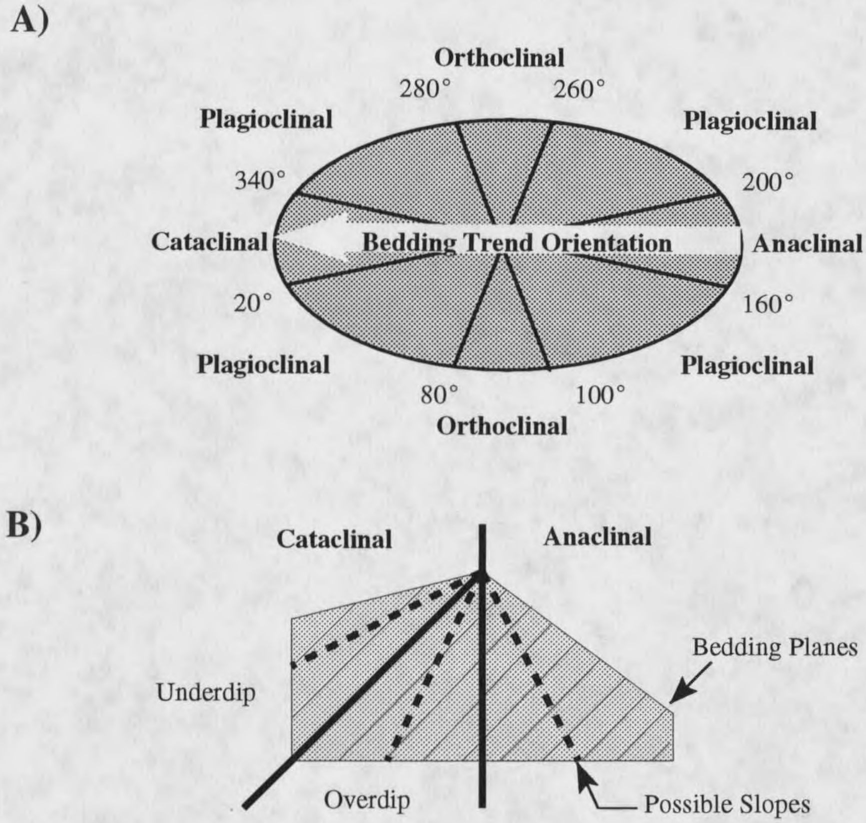

Figure 1.9. Classification of rock slopes (After Cruden, 1985, p.529). A) Topographic aspect with respect to bedding trend orientation. B) Topographic gradient with respect to bedding trend dip.

Cruden and Eaton (1987) observed that slope failures in Kanaskis Country, Alberta, Canada occur dominantly on cataclinal overdip slopes (Fig. 1.10) even though they make up less than 10% of the total area examined. A useful ratio can be created by dividing the percent of all slope failures in a particular class by the percentage of the study area that is in this class. This ratio will be referred to as the "failure per area" or FPA ratio throughout the remainder of this paper. A large FPA ratio indicates that slope failure is unusually common in the indicated slope type. A small FPA ratio indicates that slope failure is rare in the slope type class. Note that cataclinal overdip slopes have a very high FPA ratio (4.4) and are prone to slope failure (Fig. 1.10). Cataclinal underdip slopes, however, are unlikely to fail with a low FPA ratio of 0.3. In order to predict where rock slopes will fail cataclinal overdip slopes locations appear critical. For a gently deformed sedimentary terrain such as southern Yellowstone County, GIS is an appropriate tool to relate the factors (topography, lithology and discontinuities) to mapped and potential slope failures (Fig. 1.11).

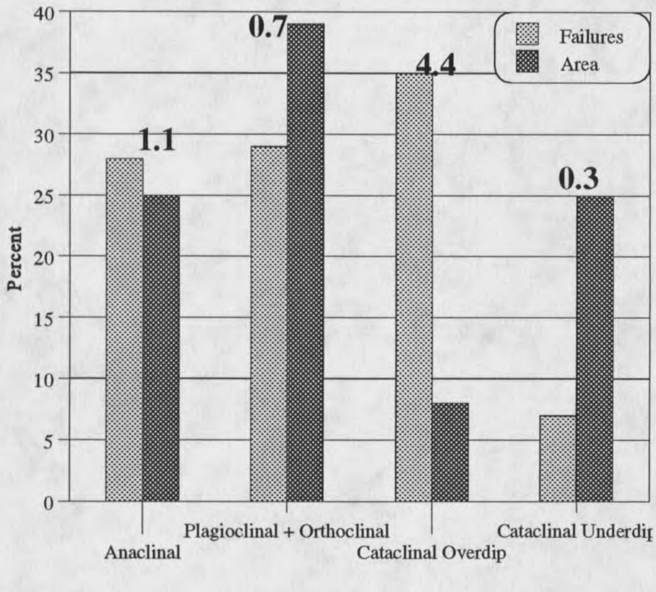

Figure 1.10. Distribution of slope failures for slope types in Kanaskis Country, Alberta, Canada. Failure/Area ratios shown (After Cruden and Eaton, 1987, Fig. 8 + 9, p.419).

A discontinuity factor which includes slope and material properties is expected to improve the prediction of slope failure locations. Slope type combined with dip should be highly correlated to slope instability (i.e. cataclinal overdip slopes most unstable and cataclinal underdip slopes most stable). Assuming slope gradient accounts for 60% of the total distinction between slope instability and slope stability then Selby's data suggests that 60% of the remaining 40% (24% of total) should be accounted for by discontinuities

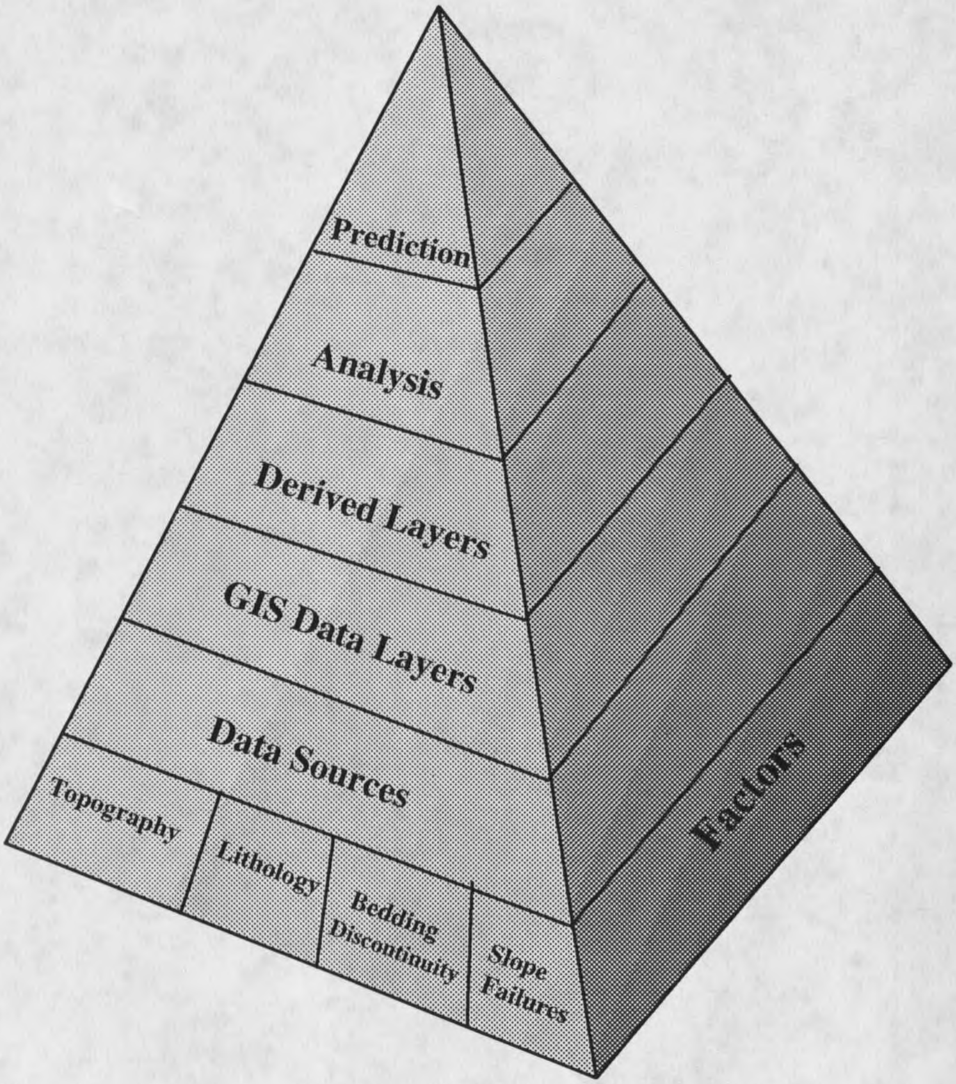

Figure 1.11. Factors for GIS stability model. Topography, lithology, bedding discontinuities and existing slope failures are foundational to this rock slope stability analysis.

(Table 1.3). The hypothesis is that slope type will account for at least half of the discontinuity effect or 12% of the total distinction between stable and unstable slopes. After observing a correlation between mapped landslide location and the mapped geologic contacts an *a posteriori* hypothesis is that the distance to a unit contact will also be significant in predicting unstable slopes.

CHAPTER 2

METHODS

The areas of potential slope failure are identified using GIS to relate the factors of slope, lithology, and discontinuities to mapped landslides. ARC/INFO is the best GIS package because of its capability to do the analysis and its availability at both the Montana State University Geographic Information and Analysis Center and the Yellowstone County Planning Department.

The GRID module in ARC/INFO is particularly suited for the analysis of continuously varying spatial data (e.g. topographic and bedding discontinuity) (ESRI, 1991). Cell operations are simpler both computationally and conceptually than polygon operations for analyzing multiple data sets (Bonham-Carter, 1994). Because the source topographic data is a 30 meter grid, no increased (finer) resolution can be gained from using a polygon model. Topography, lithology, discontinuities and mapped landslide ARC/INFO layers (Fig. 2.1) are built from the best available data sources.

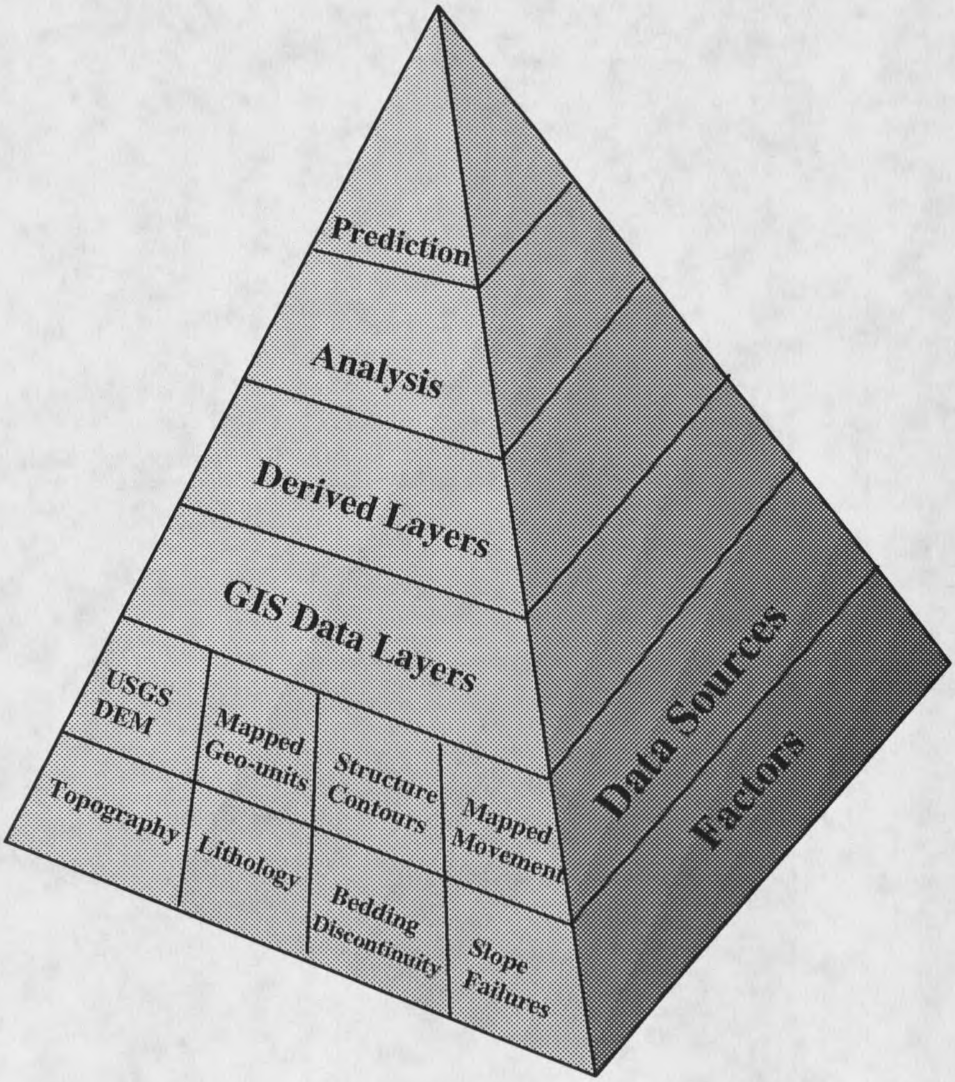

Figure 2.1. Data processing for stability analysis. Digital data (DEM) and paper maps (geologic units, structural contours and mapped movements) are the data sources used to represent the stability factors.

Data Layers

Digital Elevation Model

A Digital Elevation Model (DEM) is one type of electronically structured topographic data. The United States Geological Survey (USGS) distributes 30m DEMs that correspond to USGS 7.5-minute (1:24,000) map series. DEMs are prepared by the USGS from elevation contours or digitization of stereo models of air photographs. A DEM consists of elevation points 30 meters apart both row-wise and column-wise referenced to the Universal Transverse Mercator (UTM) coordinate system (North American Datum of 1927). The study area (Fig. 2.2) is limited by the availability of the 30m DEMs within Yellowstone County (Elassal and Caruso, 1984).

The accuracy of the DEM is based on the accuracy of the 7.5-minute contour map series, which follows the National Map Accuracy Standards. Less than 10% of the data points are in error by 1/20th of a map centimeter (1/50th inch) horizontally and 15 meters (50 feet) vertically at a scale of 1:24,000 (Thompson, 1974). DEMs contain the error allowed in the topographic source maps plus an additional unknown amount of error from the contour-to-DEM conversion. The conversion process assigns a single elevation value to every 30 m cell. A resulting error is that the actual high and low points of a surface are not necessarily included in a DEM with elevation points on a uniformly sampled grid. Thus the DEM is slightly smoother than the real surface.

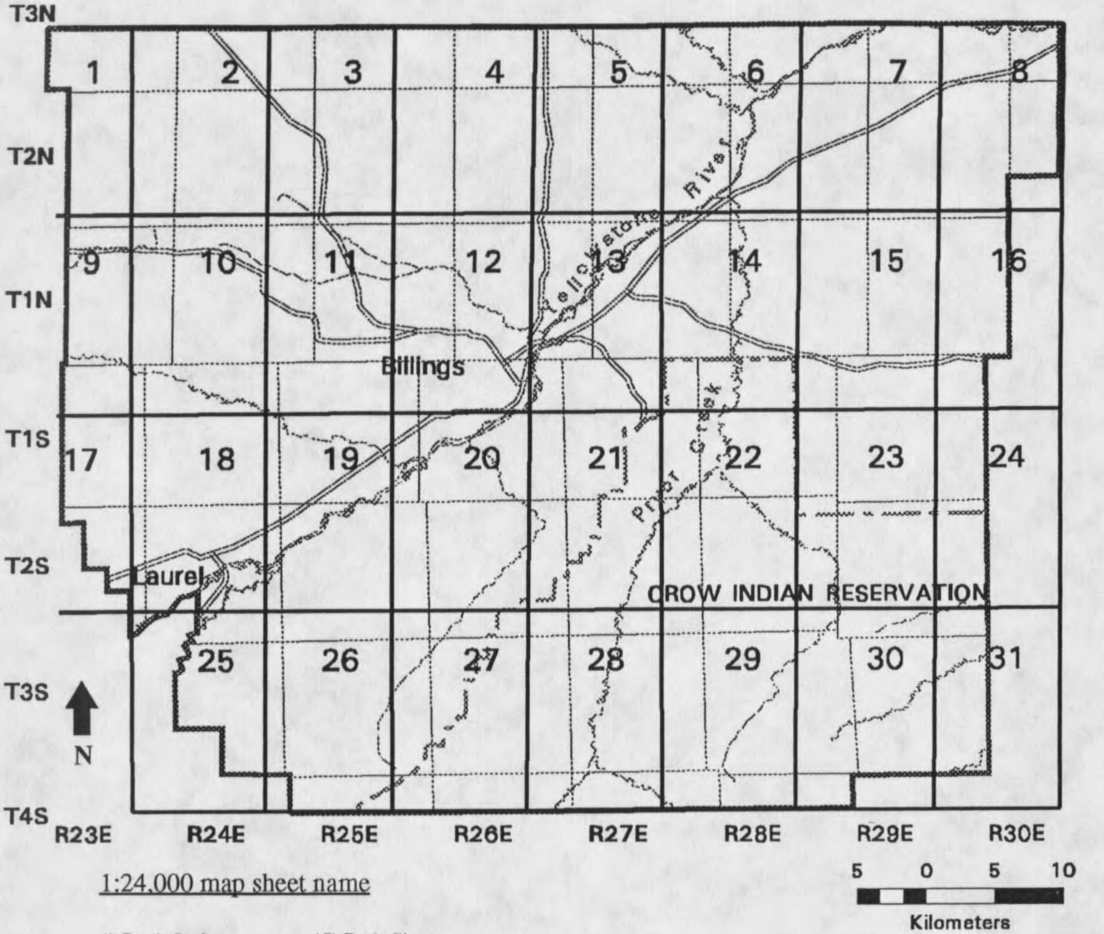

1:24,000 map sheet name

1) Rock Spring
2) Commanche
3) Acton
4) Hickson Ranch
5) Rattlesnake Butte
6) Huntley
7) Worden
8) Nibbe
9) Molt
10) Two Pine Creek
11) Rimrock
12) Billings W
13) Billings E
14) Cottonwood Creek
15) Indian Arrow
16) Gails Coulee
17) Park City
18) Lauel
19) Mossman
20)Yeagen
21) Soda Springs NW
22) Babby Coulee
23) Woody Mountain NW
24) North Telegraph Creek
25) Stella
26) Mossmain SW
27) Stratfore
28) Vale Creek Ranch
29) Soda Springs
30) Woody Mountain
31) Woody Mountain SE

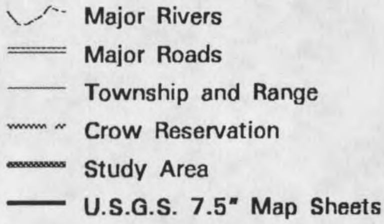

Figure 2.2. Index map of 1:24,000 DEM sheets.

The DEMs (USGS format) are converted to an ARC/INFO grid for the study area. The grid extends 0.5 kilometers beyond the study area to eliminate edge effect error within the study area. Each grid cell except edge cells has eight neighboring cells.

Roundoff error is transmitted to the grid from the DEM. Because the DEM elevation points were rounded off by the U.S. Geologic Survey to the nearest meter, artificial steps are produced in flat areas where 1 meter rise occurs over a large run. Rather than an even change of elevation along a slope, there is no change in elevation over most of the cells along the slope but at one cell the elevation jumps a meter. In steep areas where 1 meter rise occurs over a short run, each cell along a slope increases by at least 1 meter so artificial steps are not produced. Roundoff error is compounded when calculating slope gradient and aspect. Where there is artificial stepped topography the gradient over most of the cells is much less than it should be. At the steps there are narrow linear areas with a gradient much steeper than it should be.

The typical solution to this problem is to filter the elevation data by replacing each cell value with an average of it and its neighbors. Low pass filters average over a small area (e.g. 3X3 cells) and high pass filters average over a large area (e.g. 9X9 cells). A low pass filter averages everything a little but does not eliminate the stepped slopes. The high pass filter averages out the stepped slopes but also flattens out topographic peaks, ridges and valleys which are more accurately represented on the original DEM. To eliminate the artificial steps without corrupting the actual steep slopes a variable filter was needed which could average over large areas of low change in elevation without averaging large areas with high change in elevation. A customized filter was used that averaged the elevation over a varying area (Table 2.1) depending on the variation in elevation over a 9X9 cell window.

TABLE 2.1. COMPARISON OF FILTERS USED FOR SMOOTHING ELEVATIONS.

Difference in elevation (δe) over a 9X9 window	Size of window (area) used for average
$\delta e <= 20$ m	9X9 (72,900 m^2)
20 m > $\delta e <=$ 40m	5X5 (22,500 m^2)
40 m > $\delta e <=$ 80 m	3X3 (8,100 m^2)
$\delta e > 80$ m	1X1 Not Averaged

The variable filter produced the best smoothing of artificially stepped low angle slopes with least modification of accurately depicted high angle slopes. All of the filters raise the minimum elevation ~1m above the minimum DEM value (Table 2.2). The variable filter lowers the maximum DEM elevation 1.6m which is nearly as good as the 3X3 filter. The maximum difference between the variable filter and the original DEM (1X1) is 27m which is better than any of the fixed-size filters. The mean difference between the variable filter and the DEM is 1.5m which is comparable to the 5X5 filter. Thus, the error that the variable filter introduces is similar to that of a uniform 3X3 or 5X5 filter. The benefit of the variable filter is that the low angle steps are removed, unlike the 3X3 or 5X5 filters, and the high angle topography is preserved better than with the 9X9 filter.

The first data layer derived from the filtered elevation grid is slope aspect. Slope aspect is calculated from the elevations of the eight neighboring cells with the ARC/INFO ASPECT function. Cell center points to the north, south, east and west are 30 m away from the cell being calculated. ARC/INFO determines the resultant vector of each of the neighboring cells values where aspect is the direction of that resultant vector. The final grid consists of a compass direction (0 to 359 degrees from north) of a "60 m aspect" because it is effectively an average over 60 m.

Slope gradient is derived from the filtered elevation grid similar to slope aspect. Slope gradient (ARC/INFO SLOPE function) is the magnitude of the resultant vector. The derived grid of slope gradient has the value of effectively the "60 m slope" in each grid cell.

TABLE 2.2. COMPARISON OF FILTERED TOPOGRAPHIC DATA (FROM TABLE 2.1).

Filter	Minimum Elevation	Maximum Elevation	Mean Elevation	Standard Deviation	Maximum difference of Abs(DEM - Filter)	Mean difference of Abs(DEM-Filter)
1X1*	867.00	1518.00	1099.87	110.19	0.0	0.0
3X3	867.89	1516.89	1099.87	110.13	37.78	0.69
5X5	868.00	1516.16	1099.87	110.10	52.96	1.52
9X9	868.22	1514.52	1099.89	110.99	63.25	3.05
VF†	868.22	1516.44	1099.81	110.13	26.89	1.49

Note: All values are in meters. *1X1 indicates original cell value of source data. †VF = Variable sized filter

Material

Material data is stored in a grid where each cell has a value representing the dominant lithologic unit at that location. Lithologic information for the study area was compiled from several published geologic maps (Fig. 2.3, Hancock, 1919; Hancock, 1920; Knappen and Moulton; 1930 and Thom and others, 1935; Gosling and Pashley, 1973). The geologic source maps were digitized and pieced together into a single polygon coverage. Each polygon within the coverage represents a single mapped lithologic unit.

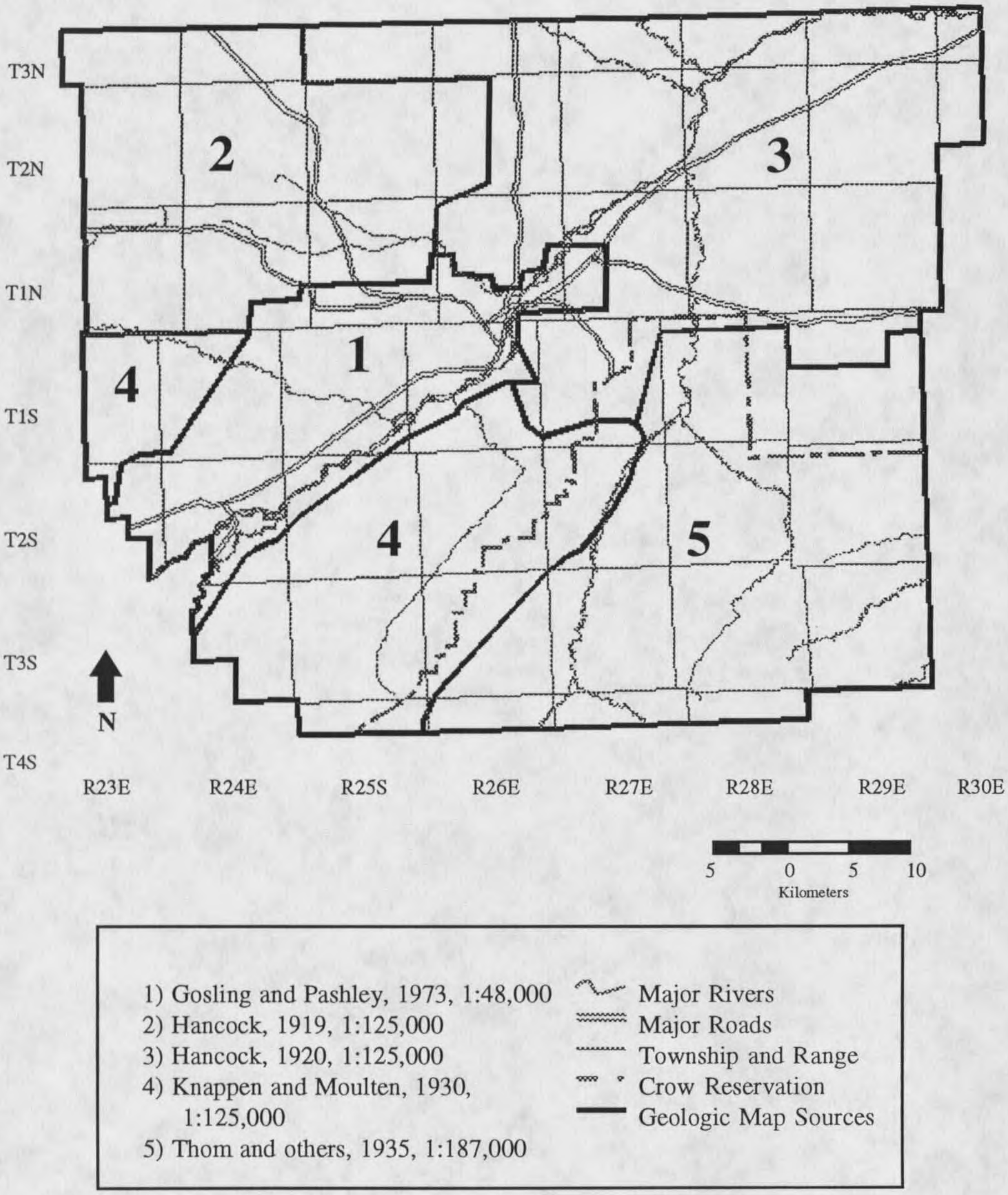

Figure 2.3. Index map of geologic sources. Publication dates and map scales are shown.

Spatial error in location varies within the polygon coverage. The greatest uncertainty is in the location of polygon boundaries representing the mapped unit boundary. Visual estimation of the map condition was made at the time of digitizing. All of the maps were folded and had an unknown amount of distortion along the folds. The amount of error due to fold distortion of the paper was determined as the distance a point on the map could move while the map corners were pulled taut and fastened. Thom and others' (1935) map for the southeast corner of the study area had severe fold creases which produce an estimated maximum ground error of 3 km in the east-west direction with a lesser amount of error in the north-south direction. Hancock's (1919) map for the north west corner of the study area was in fair condition, having an estimated maximum error of 0.2 km from distortion. The rest of the maps were in good condition (Gosling and Pashley, 1973) or very good condition (Hancock, 1920; and Knappen and Moulton, 1930) with a minimal amount of error due to map fold distortion.

Further uncertainty is inherent in the scale or resolution of the source map. The amount of uncertainty depends on the scale of the source map and digitizing error and any mapping error on the original maps. Digitizing error depends on human accuracy, the condition of the source map, and edge matching of the different source maps. The best defined source map lines (Gosling and Pashley, 1973) are mapped at the largest scale (1:48,000). A location within 0.05 cm (digitizer resolution) on a 1:48,000 scale map could vary by 24 m on the ground (one 30X30 m cell). The source map with the greatest error (Thom and others, 1935) has the smallest scale (1:187,000). A 0.05 cm digitizer error at 1:187,000 represents 94 m on the ground (three 30 m cells). The remaining three source maps of the study area (Hancock, 1919 and 1920; Knappen and Moulton, 1930) have a scale of 1:125,000. A 0.05 cm digitizing error at 1:125,000 represents 63 m (two 30 m cells) on the ground. Combined error from folds and inherent precision due to scale suggests that the total material unit boundary error ranges from little as 0.03 km, or 1 cell (Gosling and Pashley, 1973) to as much as 3 km, or 100 cells (Thom and others, 1935).

In the primary grid, each cell contains a value from digitized polygons which represents lithologic units. A reclassified materials grid was created from the lithologic units. From the reported descriptions and thicknesses the lithologic units were classified as dominantly sandstone, dominantly shale, or a mixture. Quaternary units were eliminated for each of the grids derived from lithology because Quaternary alluvium is not a consolidated lithologic unit with comparable bedding discontinuities (Fig. 2.4).

In addition to material type and the Quaternary buffer, another type of grid is created from the contacts between lithologic units (Figure 2.5). Contacts where a hard unit overlies a relatively weaker unit (h/s contacts) such as sandstone over mixed, sandstone over shale or mixed over shale, correlated visually with mapped landslides. Each grid cell was given a value relating to the distance to an h/s contact. The study area was divided into five distance classes from an h/s contact: within 125 m, greater than 125 m and within 250 m, greater than 250 m and within 500 m, greater than 500 m and within 1 km, and greater than 1 km. One hundred twenty five m is roughly an accurate location of the contact ± map condition ± digitizing error, thus 0 - 125 m indicates "on" the contact. The remaining classes represent an exponential increase in class size, conforming to the way most geologic processes behave.

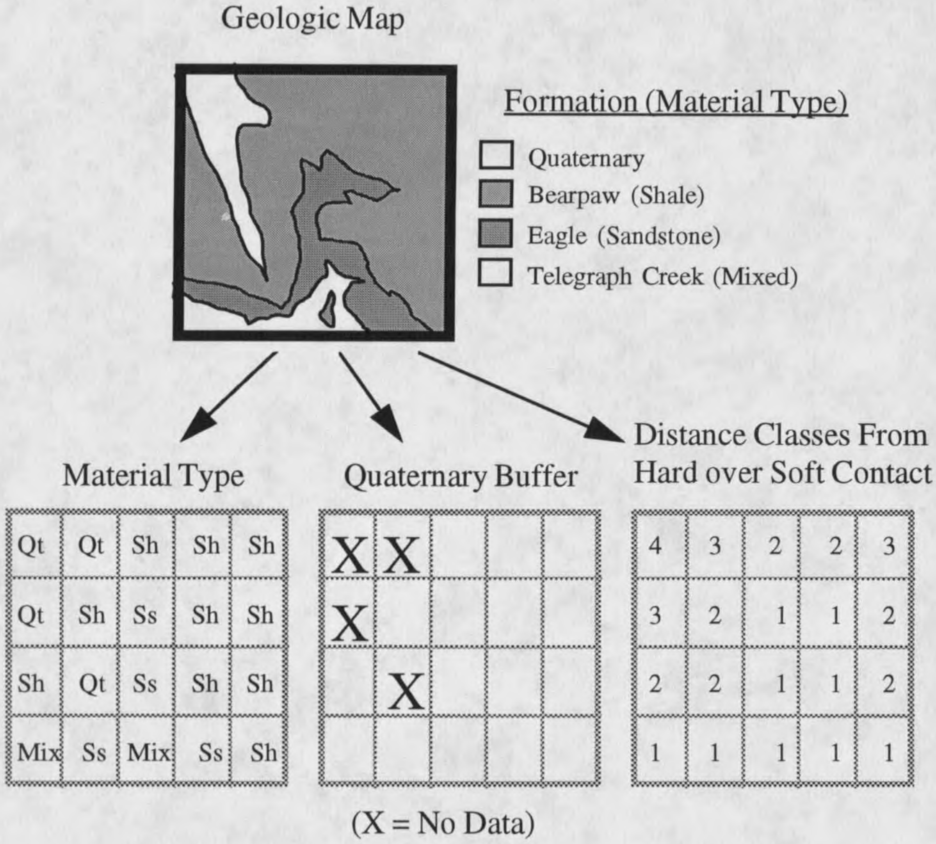

Figure 2.4. Derived Grids From Lithology. Material type is evaluated for each cell. Quaternary material are given no data values. Distances are calculated from hard over soft contacts. Note cells shown are approximately 300x300 m, actual resolution is 10 times better.

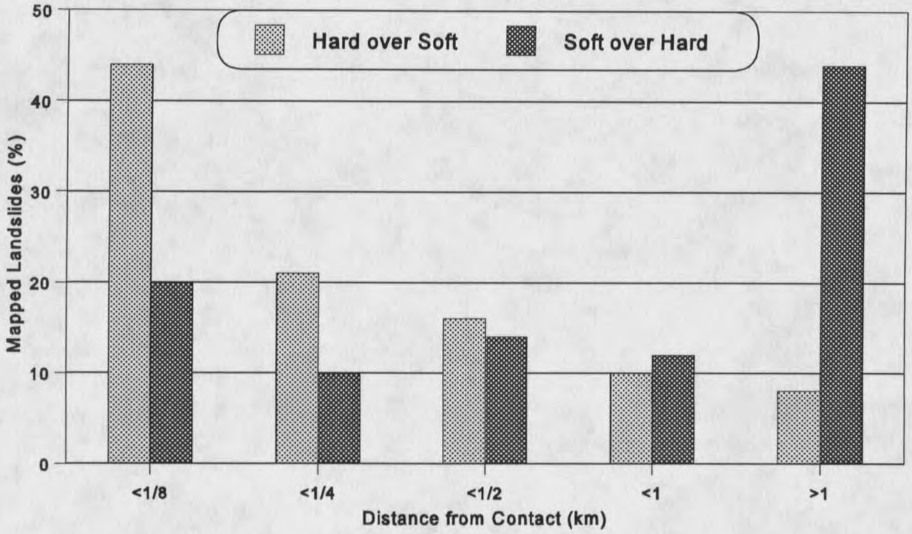

Figure 2.5. Distance of landslides to Hard over Soft contacts and Soft over Hard contacts in Yellowstone County, Montana.

Bedding Discontinuity

Rock discontinuities, such as bedding, jointing, and foliation, are usually represented by strikes and dips measured in the field. However, in this study field mapping cannot accurately represent bedding discontinuity because dip angles are very small and mapping is limited to exposed unweathered rock outcrops and there is little exposed unweathered rock. The problem of sparse dip data is not insurmountable. Dip is also characterized by structure contours. Structure contours are the elevation of a selected stratigraphic datum, either above or below sea level. Characterization of bedding discontinuities from structure contours assumes that the surface defined by the elevation contours on a stratigraphic datum within the Cretaceous is representative of the structure at the surface. The contours are inferred to be representative of surface dips because: 1) the structure deformation is uniform (outside the fault zones) from the uniform Pryor uplift to the south, 2) all of the formation and member units are continuous and conformable from the Cloverly up to the Lance (Knappen and Moulten, 1930), and 3) the original map contours appear to be inferred from surface structure (from the observed agreement of mapped strike and dips with structure contours), probably because very few wells existed at the time of mapping in the 1930's. These structure contours can be incorporated into the GIS rock slope stability analysis. Field mapping could then be focused on specific areas shown to be of concern.

Structure contours are published on the USGS geologic maps for the southern three-quarters of the study area. The contour data comes from the four geologic maps represented in Figure 2.3 excluding the map of Gosling and Pashley (1973). Contours in the south are elevations of the top of the Cloverly Formation. Contours in the north are elevations of the base of the Eagle Sandstone. Where the Eagle Sandstone and Cloverly Formations outcrop (north and south of study area respectively) structure contours are not drawn.

Oil and gas well log data provides some additional information in areas not covered by contours. The well locations are plotted on a 1:100,000 scale map from the north-south and east-west distances from section lines given on the well logs. The elevation at the top of the Eagle Sandstone was taken from the log at each location.

Both the contour surfaces and the well elevations were adjusted to the top of the Eagle Sandstone (Fig. 2.6). This datum was used because the shale-sand transition at the top of the top of the Eagle Sandstone (the prominent Rimrock sandstone as seen in Billings) is easier to identify in the well logs than the base of the Eagle Sandstone, which grades from sand to sandy shale layers. Contours at the base of the Eagle are raised 64 m to account for the thickness of the formation (Knappen and Moulten, 1930). Contours at the top of the Cloverly are raised a total of 836 m, 772 m up to the base of the Eagle plus 64 m to the top of the Eagle (Knappen and Moulton, 1930).

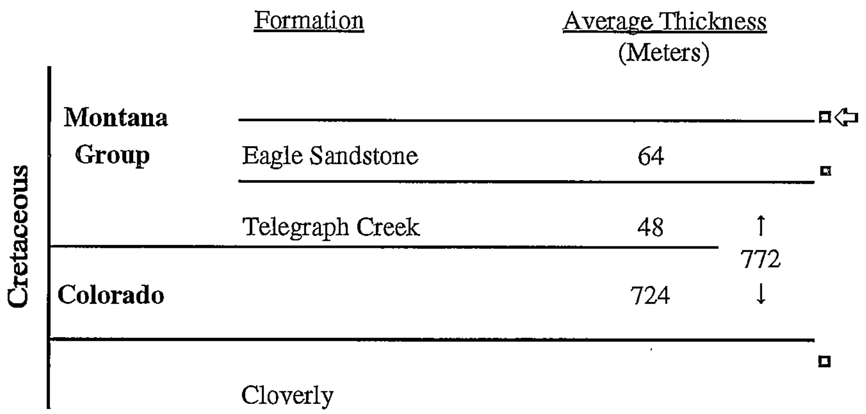

Figure 2.6. Elevation data for discontinuity surface. Note: ¤ elevation data locations, ⇦ synthesis location (From Knappen and Moulten, 1930, p. 8-9).

A grid was created by fitting a surface to the elevation points from well picks and structure contours on the top of the Eagle Sandstone. None of the interpolation methods in ARC/INFO (inverse weighted distance, spline, krig, or polynomial surface fit) were able to satisfactorily create a surface from points along the digitized elevation contours. The high concentration of points on the contours had to be decreased and additional values interpolated by hand between contours where contours were far apart, so that the final elevation points were approximately equally spaced (Figure 2.7) rather than grouped along contour lines (Eklundh and Martensson, 1995). Because the typical distance between data points is 1 km a spline interpolation is slightly more accurate than kriging (Heine, 1986). A structure elevation grid was created with a spline model within ARC/INFO.

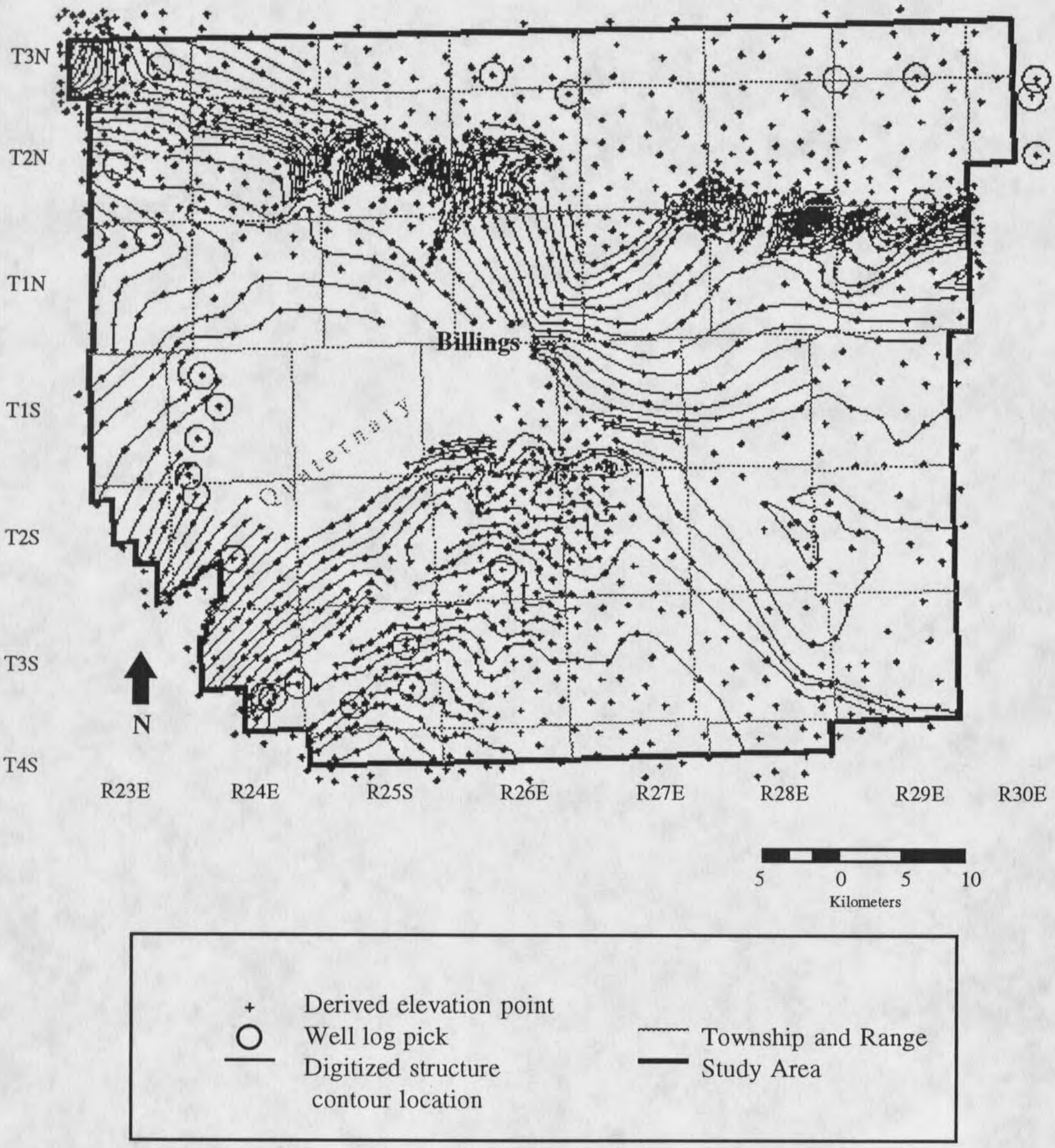

Figure 2.7. Structural elevation data points. Even spacing of data points along and between contours are used to create a non-linear biased set of data points to generate a surface. Points are derived from digitized structural contours with values adjusted to the top of the Eagle Sandstone Formation.

Areas in the Lake Basin and Fromberg fault zones have a high amount of local variation in the structural trend. The resolution of fault locations and amount of deformation is not sufficient to accurately represent the bedding discontinuity surface at the faults, thus a one kilometer (the typical distance between data points) buffer was created around each mapped fault to exclude fault regions from further structure analysis (Fig. 2.8). This excluded approximately 13% of the area. In the final discontinuity grid, each cell contains the elevation of the top of the Eagle Sandstone except for the fault buffered areas.

Mapped Landslides

The locations of mapped landslides (Wilde and others, unpublished) in the study area were digitized into a point coverage. A point coverage was used because most of the landslides are too small to be accurately represented by polygon areas (Fig. 2.9A). Although some landslides are as large as 0.5 km^2 they are digitized as points (Fig. 2.9B) because of the 1:500,000 source map scale. The small source map scale suggests a position error of ±250 m (0.05 cm x 500,000), equivalent to an area covered by eight 30 m cells. As a result, the actual point could be in one of 64 possible cells, thus an area representation of landslide location is inappropriate. The point coverage was converted to a 30 m cell grid (Fig. 2.9C). Each cell is assigned a value indicating the presence or absence of a mapped landslide. Because a landslide is represented by a single point, cells containing part of a large landslide may have a no failure value (Fig. 2.10). A cell containing a failure value will not necessarily represent either the steepest or flattest area of the landslide.

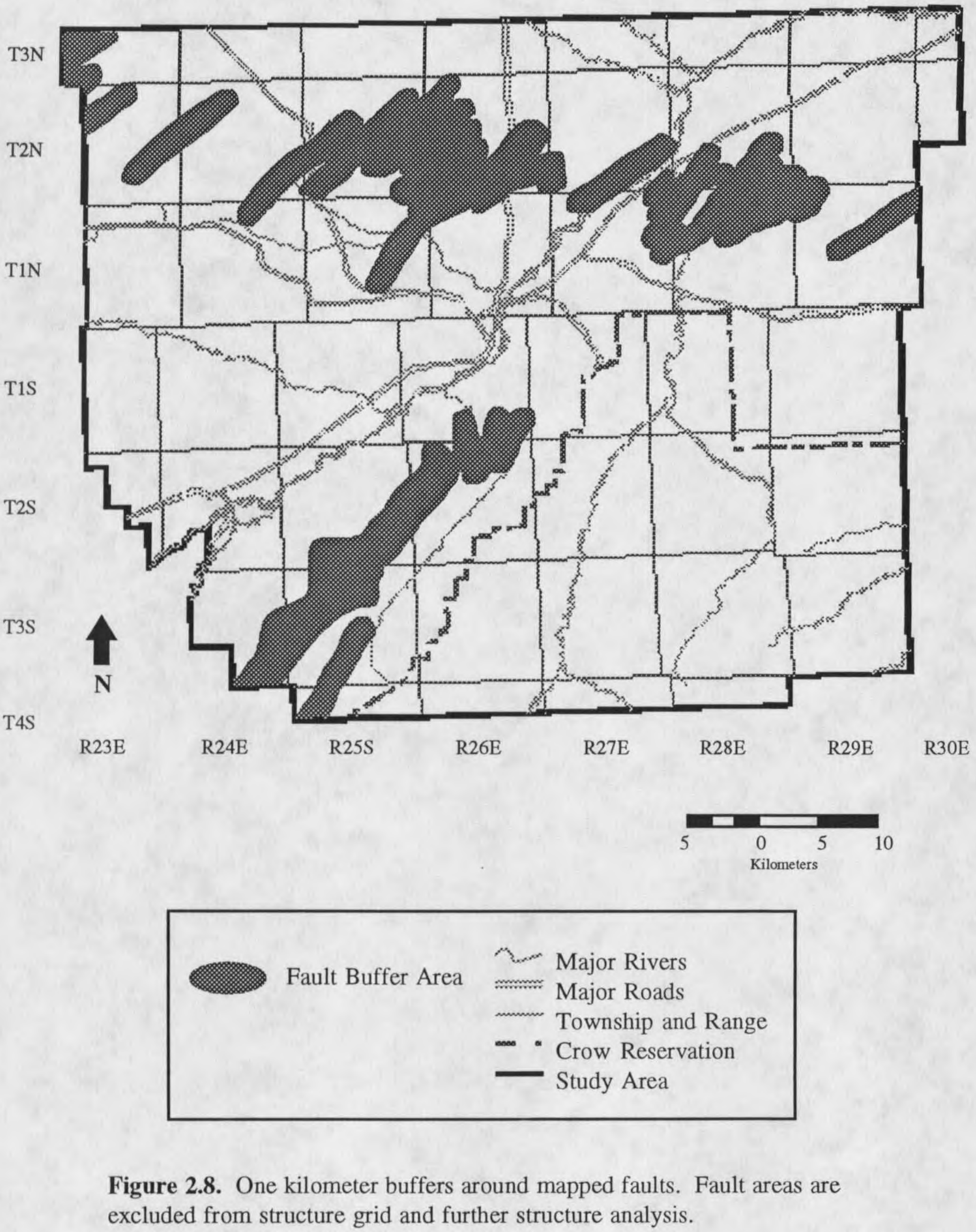

Figure 2.8. One kilometer buffers around mapped faults. Fault areas are excluded from structure grid and further structure analysis.

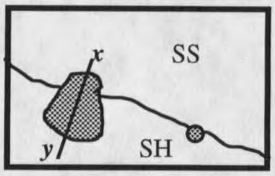

A. Mapped landslides at lithologic contact. cross-section x-y shown in Fig. 2.10.

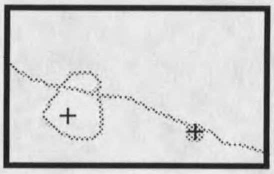

B. Digitized landslide location points.

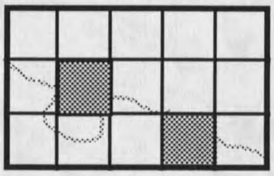

C. Grid cells containing mapped landslides.

Figure 2.9. Process of creating grid cells representing failed slope areas with A. source map, B. digitized points and C. grid cells.

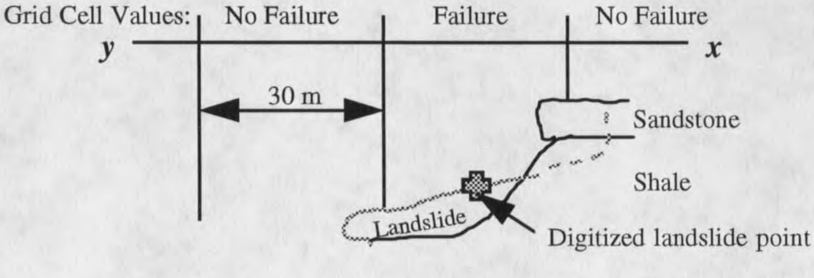

Figure 2.10. Comparison of landslide feature with derived grid of landslide occurrence. Cross section of landslide (dashed where hidden).

In addition to location error in the mapped landslide data, the lack of information on landslide type could lead to further error. Because landslides fail by many different processes each landslide point <u>should</u> have a failure type associated with it. This information did not exist in the compilation of mapped failures in Montana (Wilde and others, unpublished). In the compilation of slope failures it is likely that small rockfall failures are not included because none are shown near the Rimrocks in Billings) and that slumps, slides and flows are included in the study area. Analysis assumes that rock fall is not included on the map and other failure types are lumped together. This problem suggests an avenue for further work which may be important from a mass-movement hazard perspective.

CHAPTER 3

RESULTS: Derived Layers

The primary GIS data layers (topographic surface, material units and bedding discontinuity) can be manipulated to produce additional information more useful for rock slope instability analysis (Fig. 3.1). The derived layers of slope gradient and aspect are more useful for slope analysis than the elevation values, synthesized material types are more useful than formation names, contact distances are more useful than contact locations, and bedding dip is more useful than structure contours. One final layer (slope type) is generated as a combination of derived layers. As such, this layer has uncertainty which is compounded from error on the two source maps.

Topography

The slope gradient grid (Fig. 3.2) has the calculated percent slope value in each cell. The steep scarps of the Rimrocks and other sandstone cliffs show up distinctly. The Quaternary areas are not shown because they are not included in the study. The minimum gradient is 0% (flat) and the maximum gradient is 58.4% with a mean gradient of 5.4%.

The topographic aspect grid (Fig. 3.3) has the compass direction that slope faces in each cell. Opposite aspects along Pryor Creek and the Yellowstone river are clearly

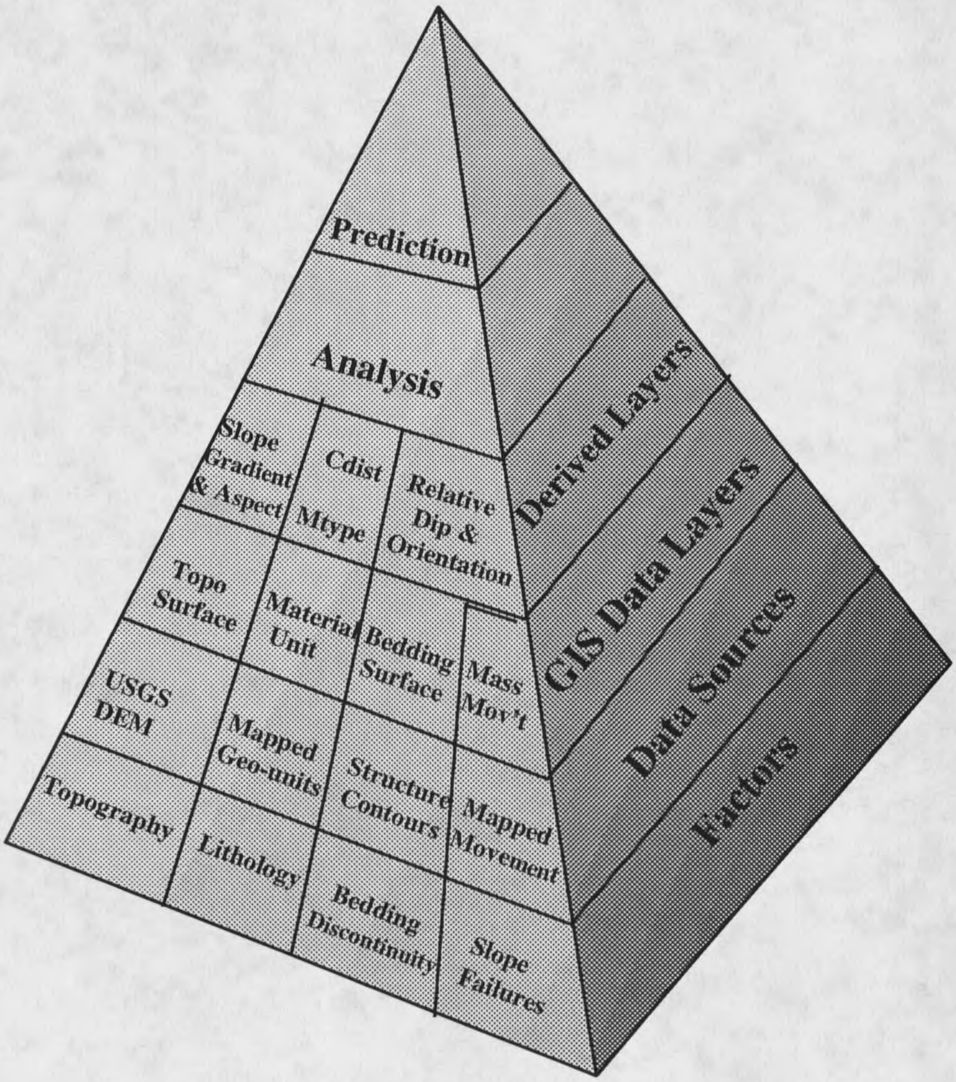

Figure 3.1. Derived layers with direct application to slope stability. Analysis and prediction are generated by mathematical and spatial operations, and by comparison of manipulated GIS data layers.

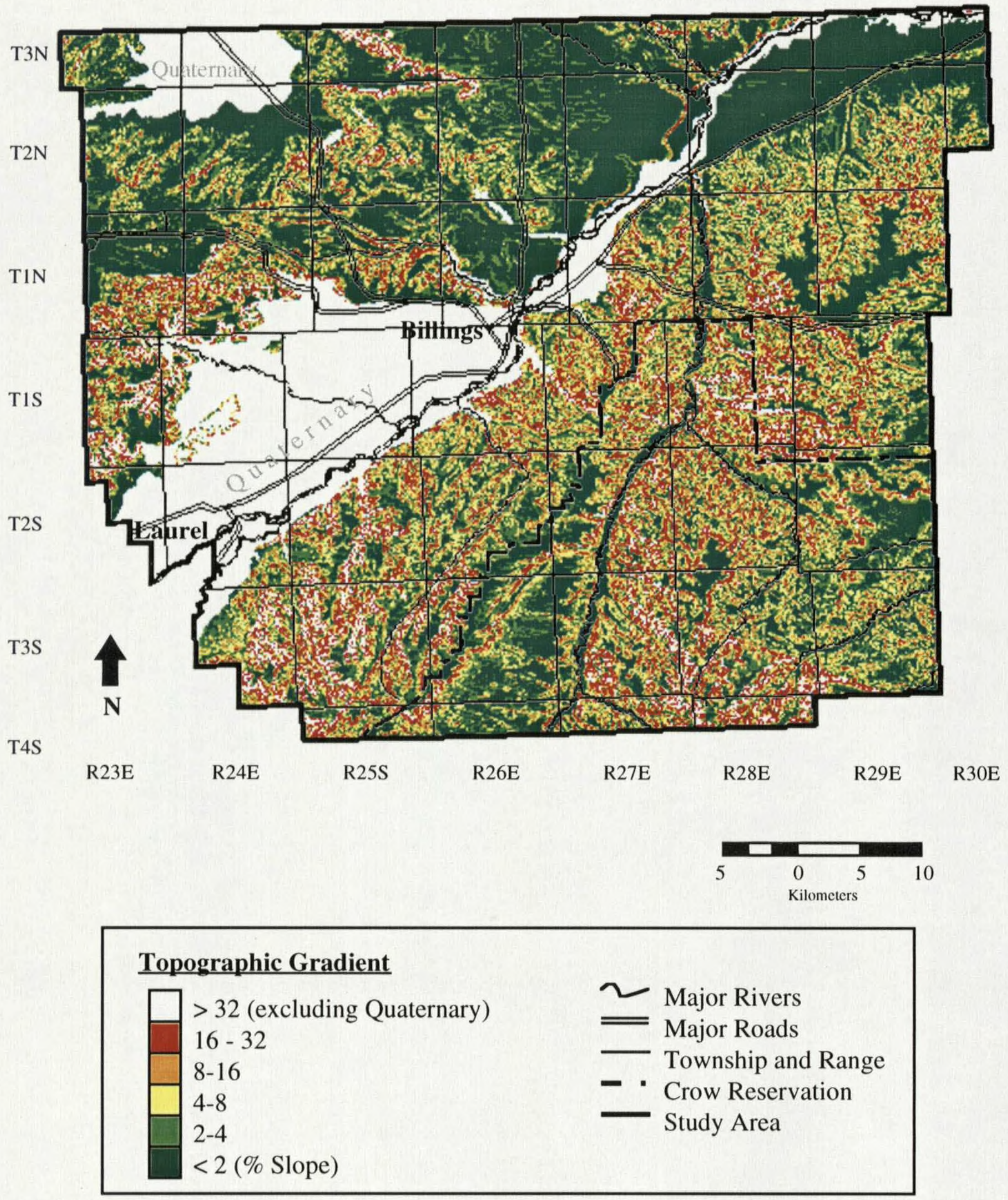

Figure 3.2. Topographic gradient derived from filtered 30 m DEM. Steep slope are evident in the dissected region south of Billings; flat areas (exclusive of Quaternary) are present northeast of Billings.

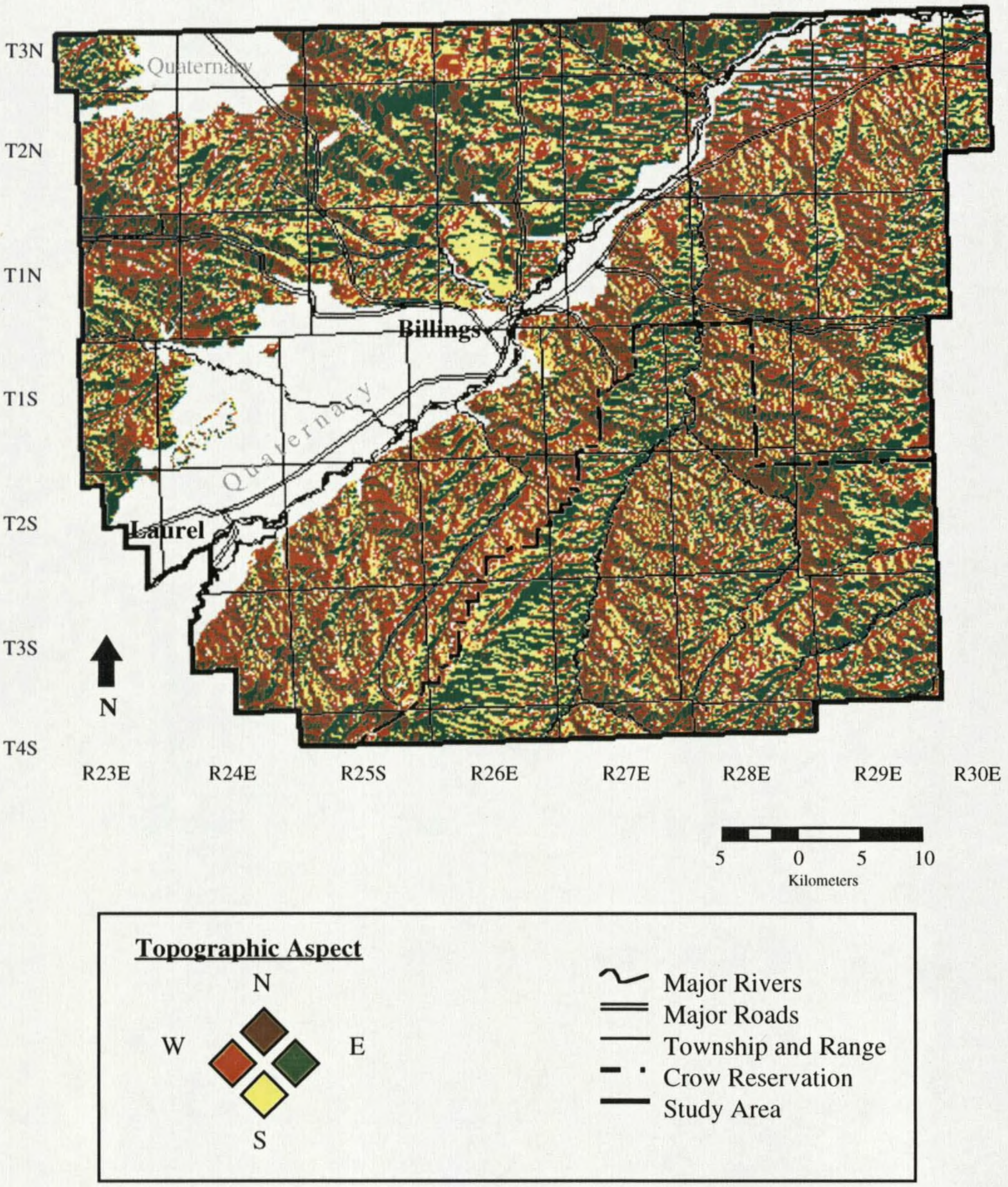

Figure 3.3. Topographic aspect derived from filtered 30 m DEM.

visible. Dendritic tributaries are also distinguishable. Aspects north and northeast are most abundant (61%) (Fig. 3.4) reflecting the structural and topographic slope away from the Pryor uplift. Southern and western aspects are less common (39%).

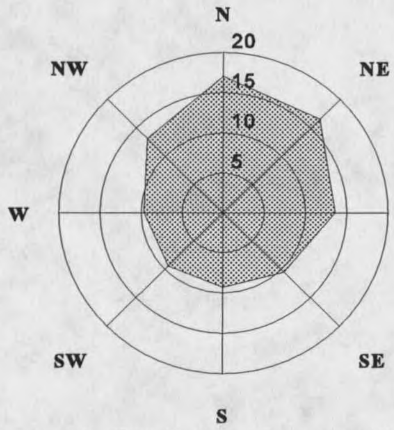

Figure 3.4. Distribution of topographic aspect (percent of area by compass direction).

Lithology

Material Type

The dominant material type in each cell was classified as either sandstone, shale or mixed (Fig. 3.5). Shale encompasses the majority (68%) of the study area, with mixed material at 20% and sandstone being the least prevalent at 12%.

Hard-over-Soft Contact Distance

The study area was divided into five classes depending on the distance from the nearest hard-over-soft (h/s) lithologic contact (Fig. 3.6). Fourteen percent of the study area is within 250 m of a h/s contact.

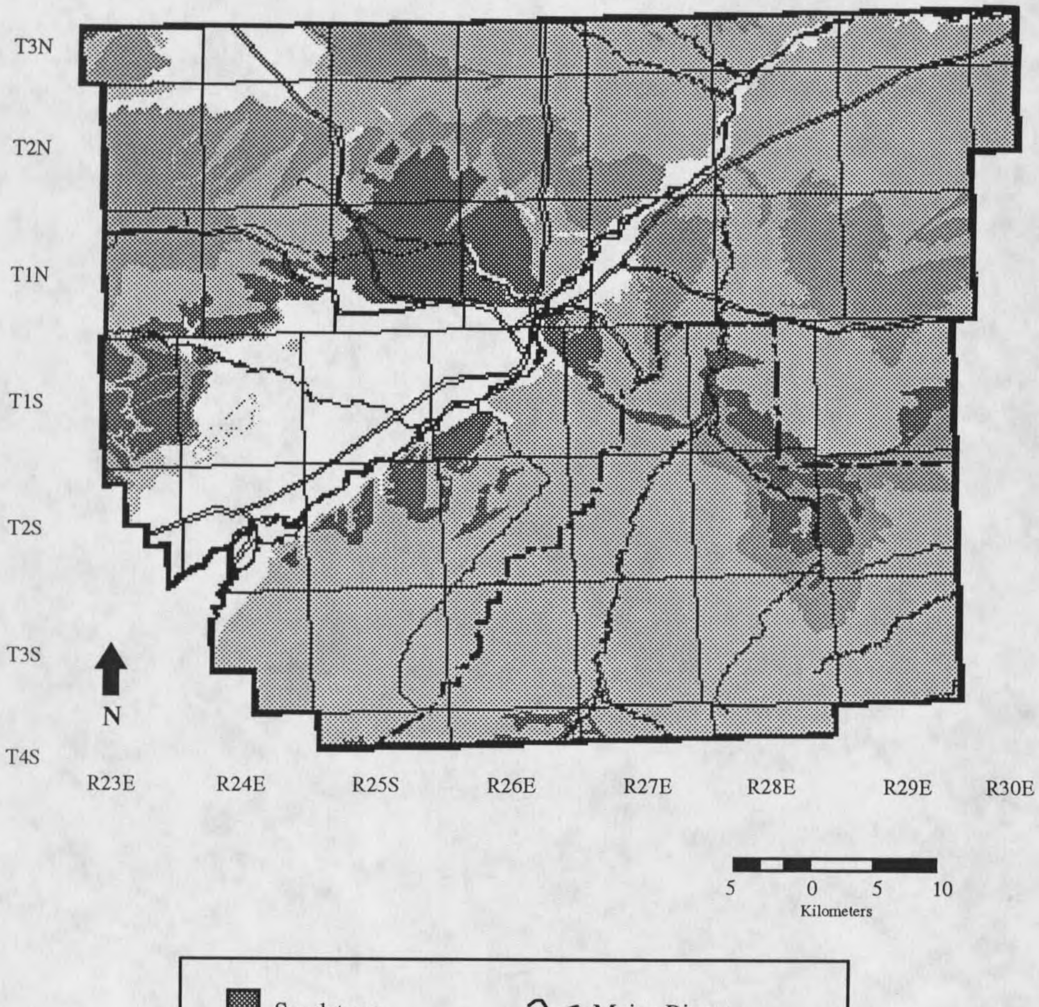

Figure 3.5. Material type. Classification derived from publications listed in Figure 2.3.

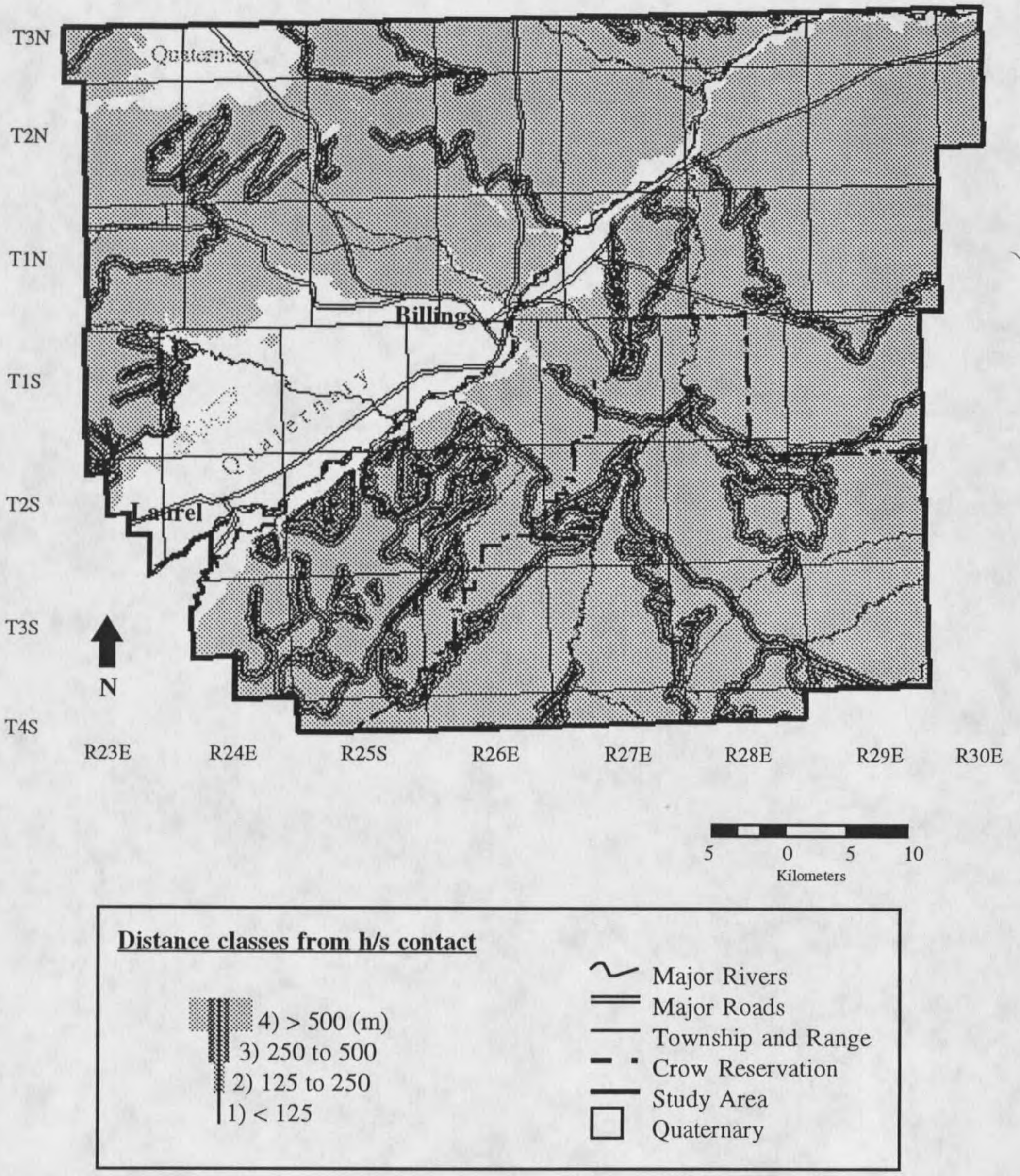

Figure 3.6. Distance classes around hard over soft contacts derived from published geologic maps.

Bedding Discontinuity

The dip of the beds reflects the steepest gradient of a Cretaceous surface, and is assumed to reflect structure at the ground surface. The assumption that the structure elevation grid (Figure 3.7) accurately represents the surface bedding trend is testable from surface structure mapping. Comparison of the structure elevation grid and fold axis of surface structure trends shows strong similarity, especially in the west central and southeast area of the study. The greatest differences are in the Lake Basin and Fromberg fault areas.

Dip gradient (Fig. 3.8) ranges from zero percent (flat) to 35% with a mean dip of five percent. Ninety percent of the dips are less than eight percent. The dip orientations (Fig. 3.9) are dominantly (85%) northwest to northeast dipping away from the Pryor uplift in the south.

Slope Type

Slope type is derived from the comparison of topographic aspect and gradient and the discontinuity orientation and dip. The study area is divided into cataclinal (topographic aspect and bedding dip are parallel and in the same direction), plagioclinal (aspect not parallel to dip), orthoclinal (aspect perpendicular to dip), and anaclinal slopes (aspect parallel to dip, but in the opposite direction) as shown in Figure 1.9. Cataclinal slopes are further divided into underdip (gradient is less than dip) and overdip (gradient is greater than or equal to dip) slopes.

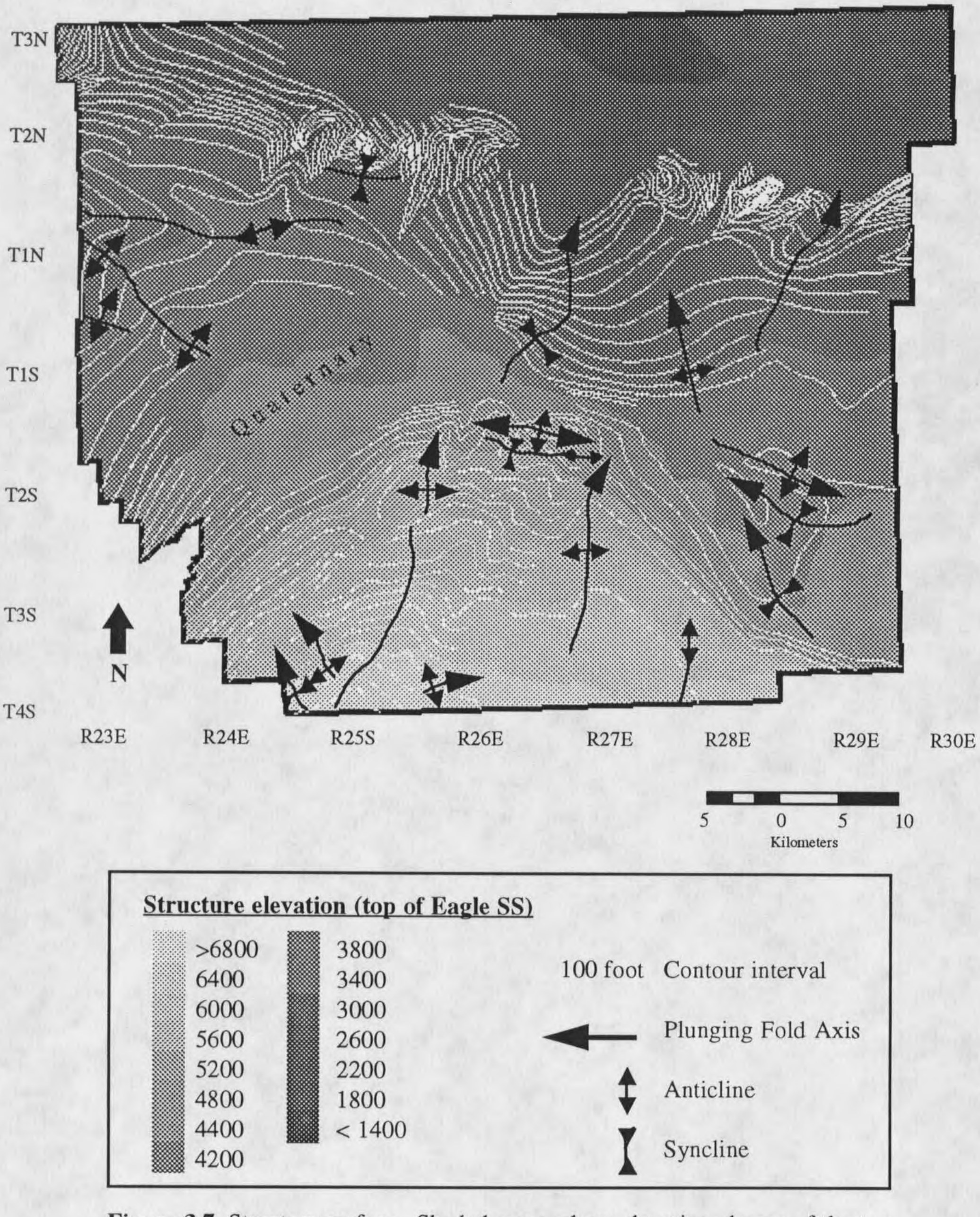

Figure 3.7. Structure surface. Shaded areas show elevation classes of the top of the Eagle SS with the digitized structure contours (white) the surface was derived from. Anticlinal and synclinal fold axis shown for comparison of surface structure trends.

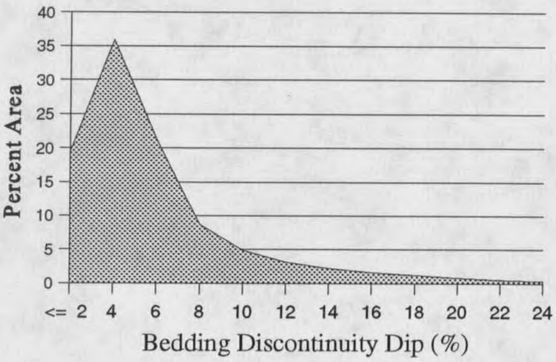

Figure 3.8. Frequency of bedding discontinuity dips. Shown in increments of two percent.

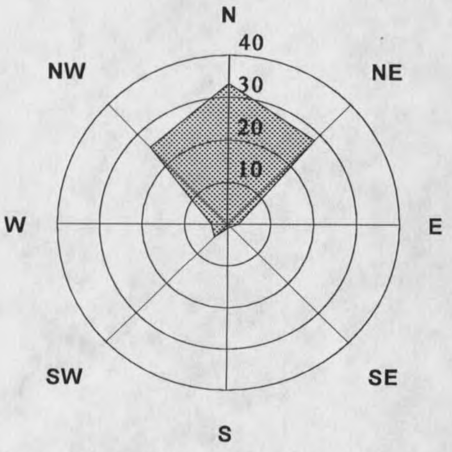

Figure 3.9. Bedding orientation trend. Shown as percent area by compass direction.

There is error in the derivation of slope type which arises both from topographic and geologic data. An unknown amount of error is introduced because topography varies within the 30m cell size. Much less error is introduced in the discontinuity orientation because structure contours vary on a scale larger than the 30m cell size. Error in discontinuity orientation exists where the orientation derived from the sub-surface structure (top of Eagle) differs from the orientation of the surface structure. The location of discrepancy is indicated by the difference between the structure grid and surface structure trends (see Fig. 3.7). How well the calculated slope type represents a given location on the ground varies by the amount by which aspect differs from calculated aspect for 30m cell and by the amount that the sub-surface dip is different from the surface dip. At the scale of this study misclassifications are likely few and minor.

Incorrect classification of cataclinal underdip and overdip can occur when comparing the topographic gradient with the bedding discontinuity dip. The degree to which calculated gradients differ from 'real' gradients and calculated dips differ from 'real' dips represents the error. The topographic gradient is likely to be on the low side of the true value because it is the resultant gradient vector from each adjacent 30 m grid cell.. The calculated gradient is an average gradient measured over 60 m because it is calculated from point elevations 30 m in adjacent grid cell. Error in the bedding discontinuity dip is low because of the broad trends in the structure contour surface. Thus, comparison of averaged topographic slope with discontinuity dip likely yields fewer overdip slopes than actually exist and more underdip slopes than actually exist. The magnitude of this error is unknown.

Figure 3.10 shows the distribution of slope types in the study area compared to a random distribution. Anaclinal, orthoclinal and cataclinal slopes have classification areas of 40° of the total 360° of arc or 11% of the total possible area. Plagioclinal slope type accounts for the remaining 240° of arc or 67% of the total area. If the distribution of slope type were random, the area for each slope type is expected to be equivalent to the percentage of the slope type classification. The percentage of total area for anaclinal, orthoclinal, and plagioclinal slope types is slightly less than the percentage expected from a random distribution and cataclinal slopes are greater than expected. Eighty-five percent of cataclinal slopes are classified as underdip slopes with the remaining 15% (2.4% of total area) classified as overdip. Even though the frequency of cataclinal slopes is greater than expected from random chance a Chi-squared of 2.40 (with 3 degrees of freedom) shows that the distribution of slope type is not distinguishable from random at $\rho < 0.05$.

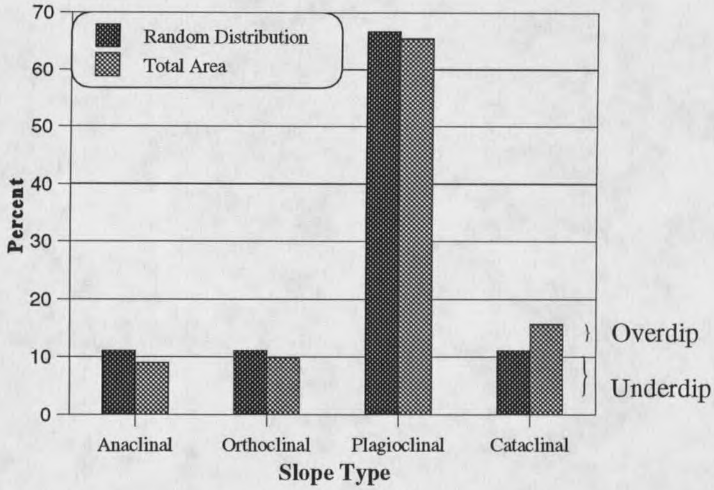

Figure 3.10. Slope type distribution compared to expected random distribution.

CHAPTER 4

ANALYSIS AND INTERPRETATION

In this chapter analysis of slope stability factors are explored qualitatively below (Fig. 4.1). Quantitative statistical correlation of the factors with slope stability for prediction is presented in the following chapter.

Derived Layers and Slope Failure Comparisons

Low gradient slopes predominate, both in the study area as a whole and in cells with landslides (Fig. 4.2). However, the percent of total area in each gradient class decreases exponentially while the percent of cells with slope failures decreases linearly. A Chi-squared of 79.11 (with 3 degrees of freedom) shows that the gradient of the landslide cells is significantly different from the gradient of cells for the total area at $\rho << 0.01$. For slopes less than 4%, the FPA ratio is 0.5 and for slopes greater than 8% the FPA ratio is $\geq$ 2.5. This relationship is as expected, steeper slopes are more prone to landslides.

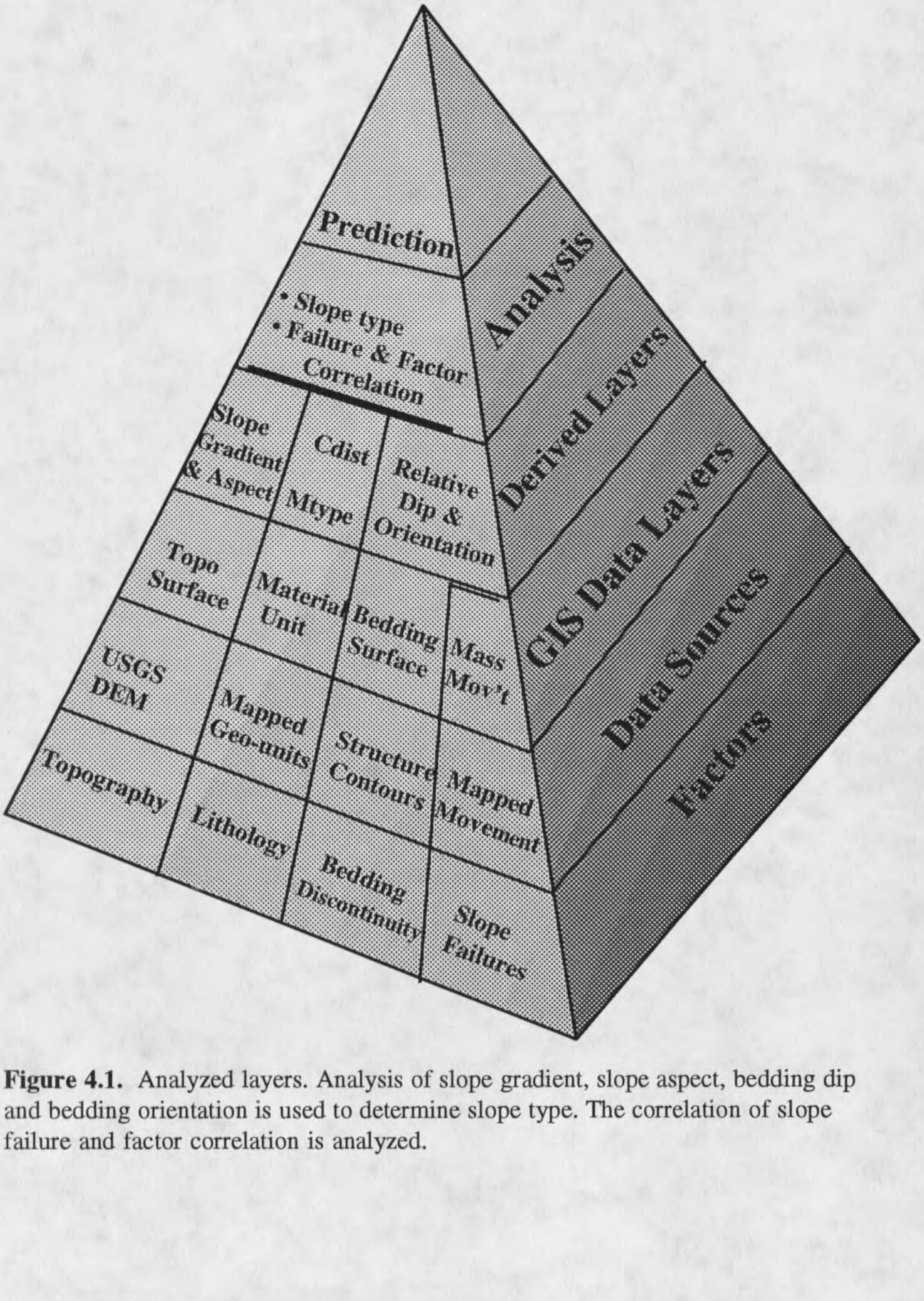

Figure 4.1. Analyzed layers. Analysis of slope gradient, slope aspect, bedding dip and bedding orientation is used to determine slope type. The correlation of slope failure and factor correlation is analyzed.

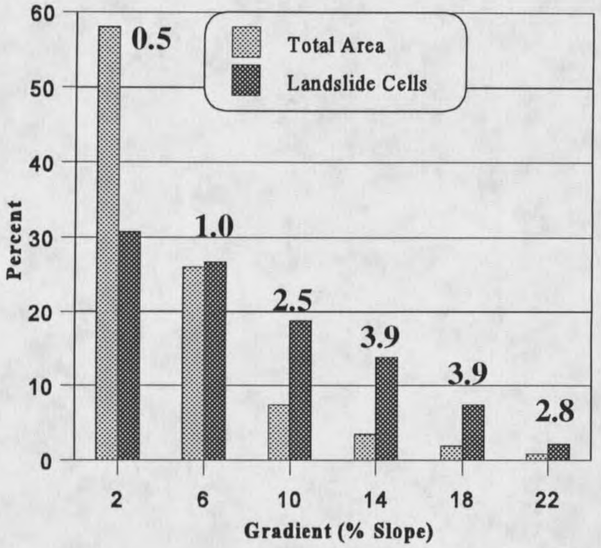

Figure 4.2. Gradient distribution of total study area and mapped landslide cells. FPA ratios are shown above each histogram class.

Distribution of material type for landslide cells is similar to that for the whole study area (Fig. 4.3). Sixty three percent of all failures occur in dominantly shale material, which makes up 67% of the study area. In both mixed and sandstone material types, the total study area in the class is lower than the percent of landslide cells. The lack of association between landslide and lithology shown by a Chi-squared = 0.98 (with 2 degrees of freedom at $\rho < 0.05$) is <u>not</u> as expected from previous studies .

Most of the study area (74%), and most of the landslide cells (64%) lie more than 1 km from a h/s geologic contact (Fig. 4.4). However, landslides occur 1.7 times more often within 125 m of a h/s contact than would be expected by chance and 1.4 times more often between 125 and 250 m of a h/s contact. As initial observation indicated, the distance to the nearest h/s contact shows a significant positive correlation (Chi-squared = 6.43 with 3 degrees of freedom at ρ < 0.05) with mapped slope failures.

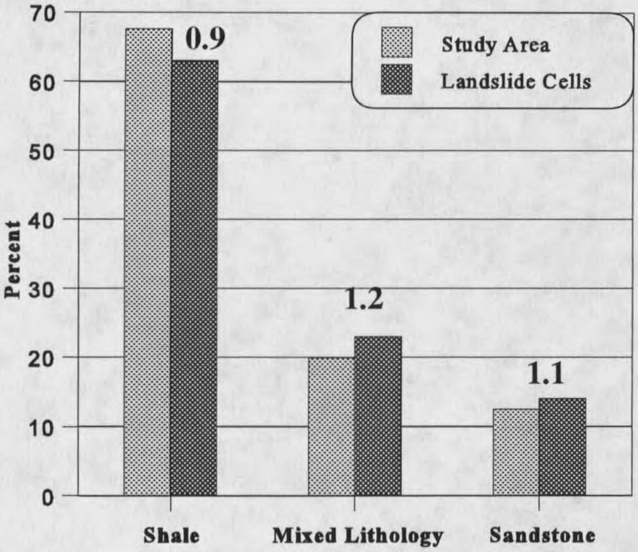

Figure 4.3. Distribution of material types for total study area and landslide cells. FPA ratios are shown.

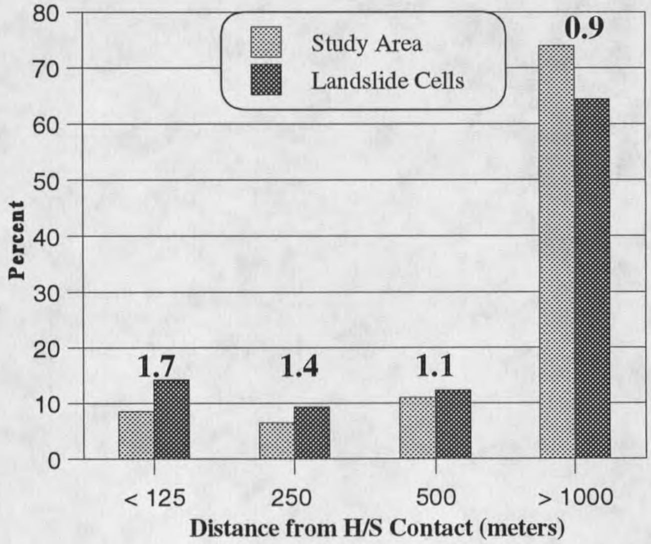

Figure 4.4. Distribution of area in distance from h/s classes for total study area and mapped landslide cells. FPA ratios are shown.

Figure 3.9 showed that the study area has more cataclinal slopes than expected, with all other slope types having fewer than expected. The FPA ratios for anaclinal, plagioclinal and orthoclinal slopes (Fig.4.5) indicates that landslides occur neither more or less frequently than expected by chance. However, on cataclinal overdip slopes, a FPA ratio of 2.1 shows that landslides occur much more often than expected by chance; and the FPA ratio of 0.7 on cataclinal underdip slopes show landslides occur less often than expected by chance (Chi-squared = 4.57 with 3 degrees of freedom at $\rho < 0.1$). The FPA ratio of the cataclinal overdip slope class indicates that slope type will be an important factor. However, the frequency of cataclinal overdip slopes is one tenth the frequency for Kanaskis Country, Alberta, Canada (3% vs. 35%) and the FPA ratio is half that for Kanaskis Country (2.1 vs. 4.4) (Cruden and Eaton, 1987). This suggests that slope type will be less than half as significant in this study than slope type was in Kanaskis Country.

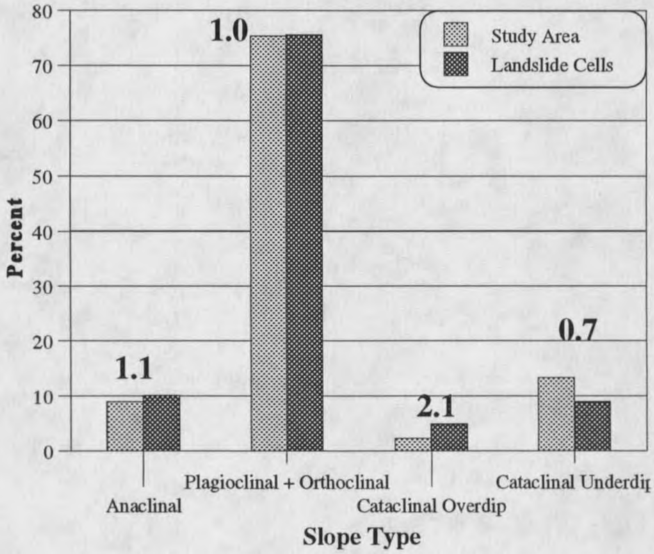

Figure 4.5. Distribution of slope type for total study area and mapped landslide cells. FPA ratios are shown.

CHAPTER 5

DISCUSSION - PREDICTION

Material type, slope gradient, distance to h/s contact and slope type have been determined for each cell in the study area and typical conditions of failed slope cells (mapped landslide locations) have been compared to typical conditions of stable slope cells (set of not failed slopes). In this chapter, statistical analysis is used to determine the most significant differences between failed slope cells and stable slope cells. The relative importance of gradient, material type, h/s contact distance and slope type for predicting slope instability will be evaluated in the statistical analysis. This analysis will test the null hypothesis that slope gradient, material type and the distance to h/s contact and slope type are not significant predictors of slope instability. Discriminant analysis will be used to determine the differences in factor characteristics between failed slope cells and stable slope cells. The differences will be used to predict how close the conditions of a given cell are to the typical failed slope cell or the probability of slope failure (Fig. 5.1). These predictions will be used to make a hazard map.

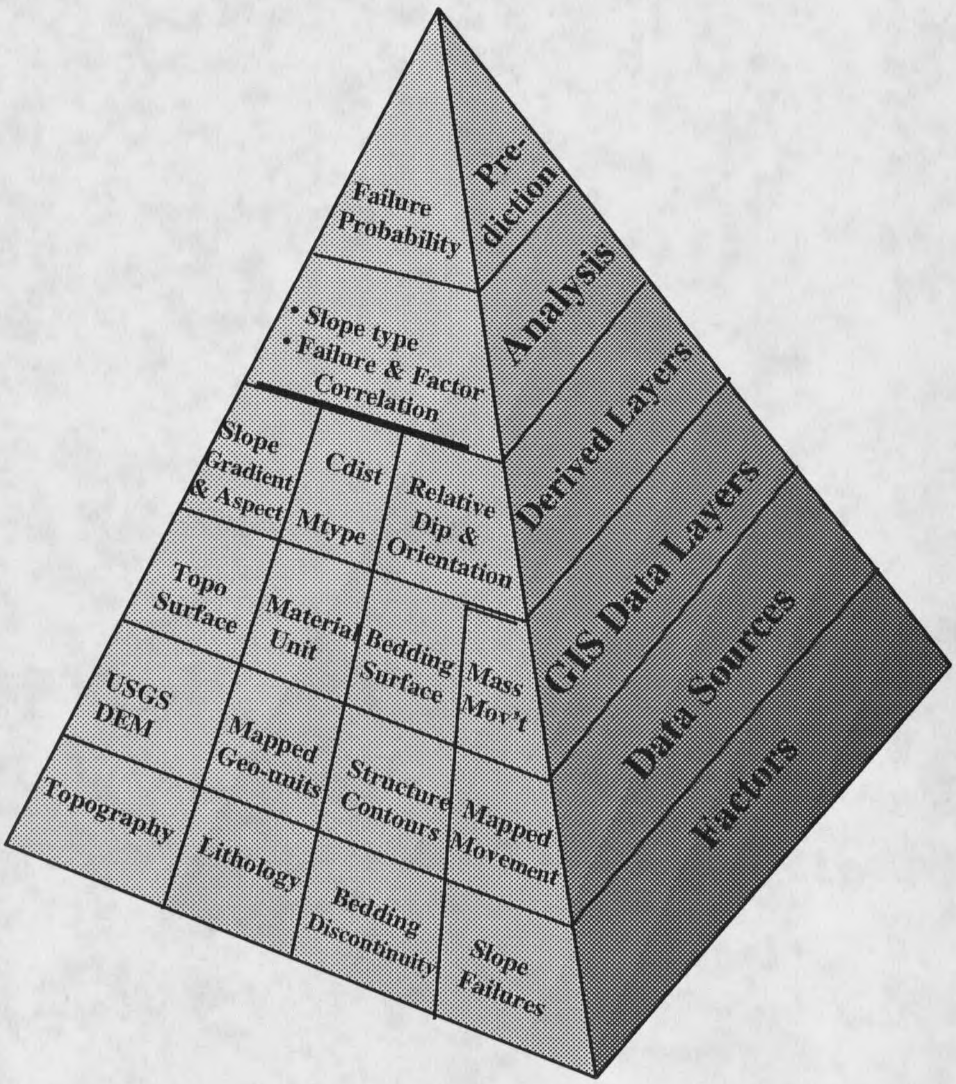

Figure 5.1. Model prediction. Statistical analysis is used to predict the probability of slope failure.

Statistical Method

Logistic regression is the ideal statistical procedure to separate a bivariate dependent variable (failure (FAIL) or non-failure (NFAIL)) with several independent variables: slope gradient (SLOPE), material type (MTYPE), distance to nearest h/s contact (CDIST), and slope type (STYPE). Logistic regression combines independent variables to optimally predict the dependent variable. However, the software packages available (SPSS, SAS and MSUSTAT) were not flexible enough to use both discrete (MTYPE and STYPE) and continuous (SLOPE and CDIST) independent variables. A hierarchical one-way discriminant function is able to create a linear combination of the independent variables to maximize the differences between FAIL and NFAIL. The discriminant function can then be used to predict probability of failure. The SPSS^{x} software package was used for this discriminant analysis.

Because there are only 157 landslide cells and over 3 million cells in the whole study area, the whole population of cells cannot be used. A smaller sample population of study area cells was used to avoid overwhelming the small number of landslide cells invalidating the statistical comparison. A minimal number of randomly selected NFAIL cells for a valid test is 3 times the number of FAIL cells or 474. Table 5.1 shows the comparison of the whole study area to a subset of 474 randomly selected cells. The random subset of points has a lower maximum gradient and a higher mean gradient. The distribution of the percent of random points in each MTYPE class is similar to the study area distribution with a maximum difference of 3% for shale. The random cells in the first three CDIST classes show lower values than the study area distribution by ~2.5%. The 4th class makes up the difference being higher by ~7.5%. The randomly selected sample population shows the slope type distribution for each class is similar to that in the study area with a maximum difference of 3% for plagioclinal slope type.

TABLE 5.1. COMPARISON OF RANDOM SAMPLE WITH TOTAL STUDY AREA. DISTRIBUTIONS OF THE PERCENT OF THE SAMPLE IN EACH CLASS EXCEPT FOR SLOPE WHERE MINIMUM, MAXIMUM AND MEAN VALUES ARE GIVEN.

	SLOPE			MTYPE			CDIST Class				STYPE				
	Min	Max	Mean	SS	SH	Mix	1	2	3	4	Ana	Orth	Plag	Cover	Cund
Random Points	1	46	5.5%	10.6	70.7	18.6	6.1	4.4	8.5	80.9	7.4	9.7	68.8	3.2	10.8
Study Area	0	58	5.4%	12.5	67.7	19.9	8.5	6.5	11.0	74.0	9.0	9.9	65.5	2.3	13.3

The first data set used in the discriminant analysis consists of the 157 cells of mapped slope failures with the associated factors of SLOPE, MTYPE, CDIST, and STYPE (Table 5.2). The second data set consists of 474 randomly located (NFAIL) cells representing the stable slope areas for the whole study area. Factors of SLOPE, MTYPE, CDIST and STYPE were analyzed. Locations of the random cells were generated using a random selector in the GRID module of ARC/INFO. A one-way discriminant analysis is robust enough to handle groups of different sizes.

The discriminant analysis incorporates assumptions about linearity, normality and homogeneity of variance-covariance. There is an assumed linear relationship among all pairs of predictors within each group. However, no simple test for linearity exists and a violation leads to reduced power rather than increased error. The size of the samples is large enough to suggest normality of sampling distributions of means. The outcome of Box's M test is insignificant at $p < 0.001$, showing the assumption of homogeneity of variance-covariance is not violated (Tabachnick and Fidell, 1989).

TABLE 5.2. DISCRIMINANT FUNCTION DATA SET DESCRIPTION.

	Distance to h/s Contact - **CDIST**				Material Type - **MTYPE**		
	0-125m	125-500m	0.5- 1km	> 1km	SH	Mix	SS
Cells w/ Failed Slope **FAIL** (157)	30	27	26	90	137	27	10
Random Cells **NFAIL** (474)	29	21	40	383	334	88	50

Continued

Topographic Gradient - **SLOPE** (Percent)

<= 2	2 - 4	4 - 6	6 - 8	8 - 10	10 - 12	12 - 14	14 - 16	16 - 18	> 20
35	30	18	22	13	14	12	7	5	7
253	85	60	29	16	12	8	4	2	1

Statistical Analysis

In the first step of the discriminant analysis, SLOPE is used to separate FAIL and NFAIL. Slope is a strong predictor, which accounts for 77.9% of the variance in the discriminant function separating FAIL and NFAIL (Table 5.3). CDIST is also important in separating FAIL and NFAIL and is included in the second step of the analysis. CDIST alone accounts for 19.5% of the variance in separating FAIL and NFAIL. SLOPE and CDIST together accounted for 97% of the discriminant variance. The third step includes MTYPE in the analysis. By itself MTYPE has lower importance when trying to separate FAIL and NFAIL (2.6% of the variance). The factors SLOPE, CDIST and MTYPE together account for all the variance in the discriminant function's separation of FAIL and NFAIL.

TABLE 5.3. RESULTS OF STEP-WISE DISCRIMINANT ANALYSIS.

Step	Factor Entered	Factors Remaining	Variance accounted for by factor	Cumulative variance accounted for
1	SLOPE	MTYPE, CDIST, STYPE	0.78	0.78
2	CDIST	MTYPE, STYPE	0.19	0.97
3	MTYPE	STYPE	0.03	1.00

The factor STYPE is statistically insignificant when trying to separate FAIL and NFAIL. When STYPE is included in a discriminant function with SLOPE, MTYPE and CDIST the model correctly classifies only 73.2% of the total dependent variable (both FAIL and NFAIL); as compared to 74.9% without STYPE. STYPE is dropped from consideration because it does not add to the separation of NFAIL and FAIL. With STYPE included, the discriminant function classifies input FAIL locations as FAIL 6% better than without STYPE (Table 5.4). Without STYPE, the discriminant function classifies input NFAIL as FAIL 6% better than with STYPE. Correct classification of input NFAIL locations is more important because NFAIL contains a larger sample and less likely to be incorrectly classified. Input FAIL locations are less accurate because of a smaller sample size, and are more likely to be incorrectly classified because of the 1:500,000 map scale.

Ideally FAIL should represent critical threshold conditions *prior* to failure in order to best predict potential failure conditions. Because a data set of slopes at threshold conditions is impossible to obtain, the best that can be done is to project failed slopes back to what their pre-fail threshold conditions were. This attempt is a common practice where the study area is small and the information is critically needed. In a regional analysis such as this, with a digital elevation resolution of 30 m, field analysis of each failed slope would have been necessary for such reconstructions.

TABLE 5.4. COMPARISON OF ACTUAL GROUP MEMBERSHIP AND PREDICTED GROUP MEMBERSHIP OF DISCRIMINANT FUNCTIONS WITH STYPE AND WITHOUT STYPE (BOTH FUNCTIONS INCLUDE SLOPE, MTYPE AND CDIST).

	Comparison of group membership of discriminant function					
	A. with STYPE			B. without STYPE		
	Predicted NFAIL	Predicted FAIL	Total	Predicted NFAIL	Predicted FAIL	Total
Actual NFAIL	76%	24%	100%	80%	20%	100%
Actual FAIL	32%	68%	100%	38%	62%	100%

The final discriminant function was calculated with total overlap between predictors tested as Chi Square equal to 169.89 (with 3 degrees of freedom at $p < 0.01$) which shows a reliable relationship between groups and predictors. One hundred percent of the between-group variability is also accounted for. Results of the analysis are used to produce figure 5.2, where the frequency distributions are plotted for the discriminant scores for FAIL and NFAIL. Separation of FAIL and NFAIL is fairly clear at both tails of the graph. Group centroids (means) are shown.

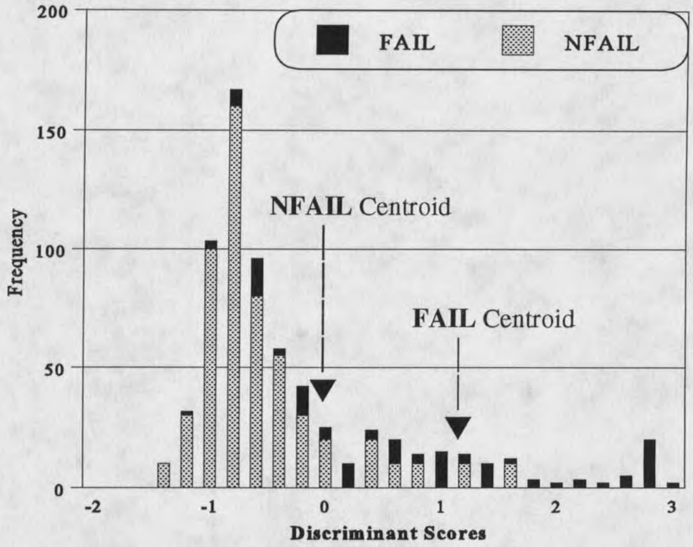

Figure 5.2. Discriminant function histogram of FAIL and NFAIL.

Correlations between predictors and the discriminant function is shown in Table 5.5. The loading correlation value indicates the correlation of the predictor variable with the discriminant function and the within group correlation shown on the right side of Table 5.5. SLOPE has the highest correlation (0.89) to the discriminant function and is the best predictor for distinguishing between FAIL and NFAIL. The positive correlation signifies that the likelihood of FAIL increases with higher SLOPE. FAIL slopes are steeper (mean gradient = 9.1%) than NFAIL slopes (mean gradient = 4.2%). Within-group correlations show that SLOPE is practically independent of MTYPE and CDIST.

TABLE 5.5. RESULTS OF DISCRIMINANT FUNCTION ANALYSIS OF STABILITY FACTORS.

Predictor variable	Loading correlation of predictor variable with discriminant function	Within-group correlations among predictors: SLOPE	MTYPE	CDIST
SLOPE	0.89	1.00	-0.04	-0.12
CDIST	-0.53		1.00	-0.08
MTYPE	-0.16			1.00
canonical R	0.48			
Eigenvalue	0.30			

CDIST has a correlation of -0.53. The negative correlation indicates a decrease in the likelihood of FAIL with an increase in CDIST. The CDIST is closer for FAIL (mean value between 250 and 500 m) than NFAIL (mean > 500 m). Within-group correlations show CDIST has only minor correlation with MTYPE or SLOPE.

MTYPE has the lowest correlation (-0.16) to the discriminant function. The negative sign does not indicate a direction of correlation because material types are discontinuous classes. MTYPE of shale favors FAIL where sandstone slightly favors NFAIL. Within-group correlations show MTYPE has negligible correlation with CDIST and SLOPE.

SLOPE and CDIST are the dominant variables in separating FAIL and NFAIL and therefore are also the best predictor variables. All the predictor variables are shown to be independent of each other (Table 5.5). The discriminant function correctly classifies 75% of the input NFAIL and FAIL. This outcome is 25% better than an expected random classification.

Slope Failure Prediction

The coefficients of the discriminant function were used to predict the probability of failure. The probability of FAIL calculated for the dependent variable of the input data set is listed in the Appendix. The discriminant function created from the sets of FAIL was used to evaluate the whole study area. Cell conditions of SLOPE, MTYPE and CDIST were entered into the discriminant equation and the probability of FAIL was calculated (Fig. 5.3).

The probability of FAIL distribution shows the strong correlation between high probability and steep gradients (see Fig. 3.3) as expected from the significance of SLOPE in

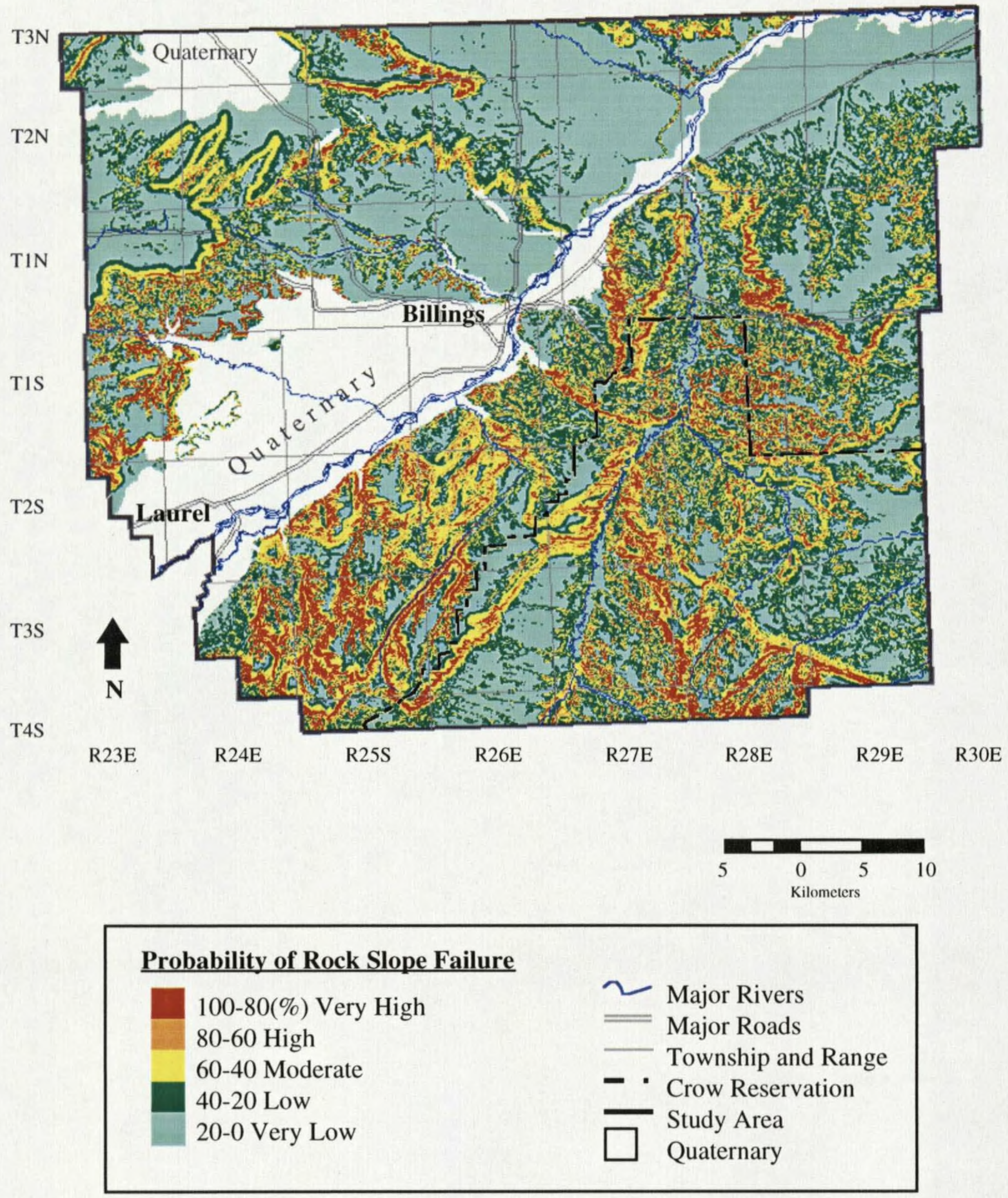

Figure 5.3. Probability of rock slope failure for southern Yellowstone County, Montana.

the statistical analysis. Hard-over-soft contacts have noticeable stripes (compare to Fig. 3.6) with a higher probability of failure. Material type is indistinguishable in the probability of failure consistent with its low significance in the correlation of MTYPE and the discriminant function.

CHAPTER 6

CONCLUSION

Outcome of Hypothesis

A Priori

STYPE is insignificant as a discriminator of FAIL and NFAIL and should not be used to predict instability in Yellowstone County contrary to the findings of Cruden (1985). The insignificance of STYPE in this study does not mean that slope type is insignificant in causing slope instability. One possible explanation for the insignificance of slope type as a predictor of slope instability is that the physical nature of the study area is below a threshold level at which STYPE becomes a significant predictor. The topographic and structure relief of Cruden's study area in the Canadian Rockies of Alberta was more pronounced than this study in the northwest Great Plains. Possibly if there were more pronounced topographic and structure relief, slope type would be a better discriminant.

Another possible explanation of the insignificance of STYPE in this study is the regional generalization of this study. The method of calculating STYPE from digital elevation and a digital structure surface for 30 m cells might have worked in Cruden's study area with more pronounced topographic and structure relief.

A Posteriori

Further investigation of the visual correlation of failures with lithologic contacts did show that h/s contacts (CDIST) correlate with instability (FAIL). CDIST accounted for nearly 20% of the total discriminant variance in this study. Knowing where h/s contacts are is important in understanding slope instability hazard in Yellowstone County, Montana. Mechanically the correlation of h/s contacts and instability is logical in that an underlying weaker unit will erode faster than an overlying resistant unit, creating slope failure potential.

Error Estimation

Generalization from sampled data such as the 30 m topography grid is only one type of error in this study. Understanding all the error is important when interpreting the results of the analysis. Error is associated with each data set, this error is multiplied when multiple data sets are combined, and additional error is introduced with every data manipulation. Figure 6.1 shows an inverted pyramid, increasing in size with successively higher layers to represent the incorporation of additional error at each level of this study. The pyramid is balanced on level 1 - the factors used in the model. Not using a factor critical to slope stability would clearly introduce error in predicting slope failure. The rationale for the use SLOPE, MTYPE, CDIST in the predictive model is based on a literature review developed in Chapter 1. Rejection of STYPE is based on the inability to separate FAIL and NFAIL (Chapter 5). The use of other factors such as hydrology, structure discontinuities, aspect and triggers is also discussed in Chapter 1. All error sources contributed to the inability to accurately distinguish FAIL and NFAIL cells thus factor error cannot be estimated.

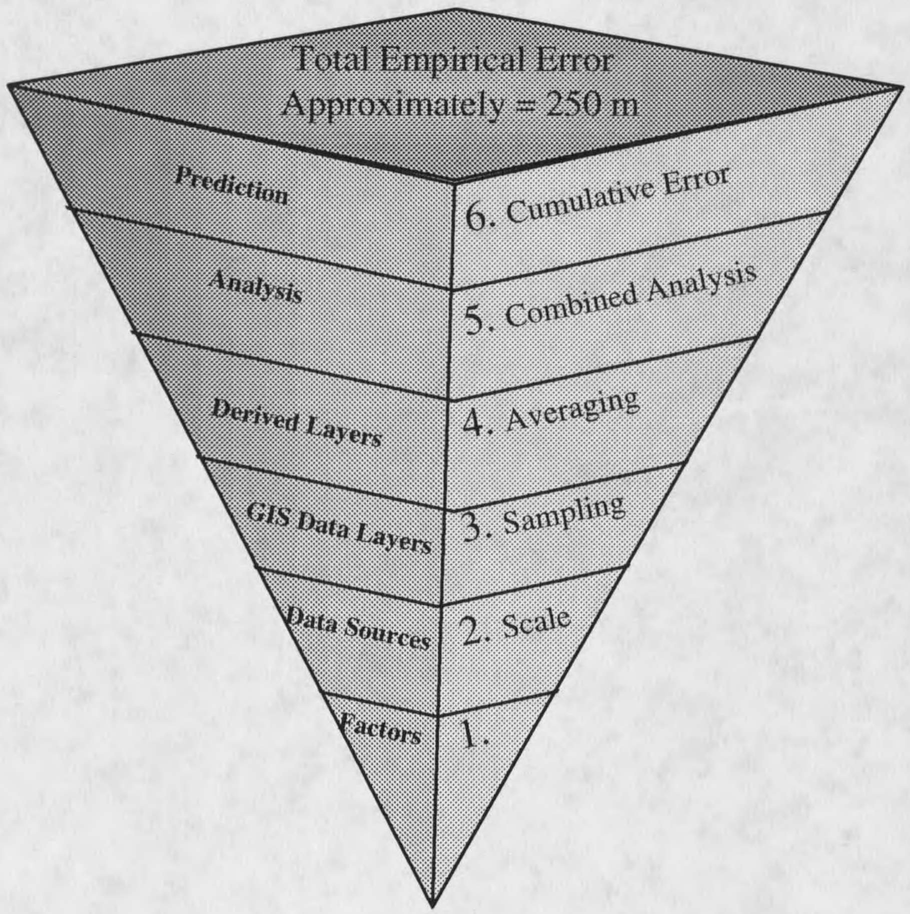

Figure 6.1. Summary of error accumulated at each level of the analysis. Error from the initial selection of factors in level 1 is added to with further analysis. The total amount of error is empirically determined to be approximately 250 m (see text for method of estimation).

Level 2 of Figure 6.1 represents the error introduced from the data source used to represent each factor. This level of error includes resolution error due to the scale of the data sources which is discussed in Chapter 2. For SLOPE there is a DEM resolution of 30 m at this level. MTYPE, CDIST and structure contours for STYPE come from geologic maps with various scales but the majority have a resolution error of ±63 m due to map scales of 1:125,000. For FAIL the mapped landslide locations have a resolution error of ±250 m due to the map scale of 1:500,000. Much of the inability to accurately predict FAIL cells results from this resolution error of ±250 m (±8 cells) in the location of mapped landslides and the resulting misassignment of low slope gradients to FAIL cells.

Level 3 (Fig. 6.1) indicates that on top of the resolution error from data scale there is error from conversion of the source data to GIS data layers. For SLOPE there is effectively no error in converting the DEM because it already is a grid format. MTYPE has a limited unknown amount of error from digitizing. Error is also introduced due to conversion of the lithologic units to material classes of SS, SH and MIX. This error averages the variation in a lithologic unit to the dominate material type for the whole unit; therefore, the amount of error is greatest in varied units and least in homogeneous units. In converting the lithologic maps to GIS data an additional amount of error of less than 30 m is introduced by sampling a lithologic area to a 30 m grid. Sampling error occurs only along the contacts where two or more material types in one grid cell are converted to the major material type. The additional added error in level 3 varies within limits. In converting data sources to GIS data layers the factors are classified into 30 m cells which reduces variability within 30 m and adds 30 m to the resolution error of level 2.

Error added at level 4 (Fig. 6.1) arises from averaging calculations for slope, aspect and filtering on 30 m grids. The topographic grid was filtered to smooth out artificially stepped data. This filtering allowed for smooth slope and aspect calculations but also introduced error. The error from the filtering process is described in Chapter 2 and summarized in Table 2.2. Additional error in calculating SLOPE is introduced in calculating slope from a 30 m grid. The slope value determined for a 30 m cell is a vector calculation of elevations from the surrounding cells. Therefore, the slope value is approximately a 60 m average slope. Average gradients are between actual steep gradients and actual gentle gradients that exist within the grid cell. Topographic aspect is determined as the direction of the filtered, averaged slope. The error in slope and aspect calculations is on the order of 60 m from averaging, but exact locations and amounts are unknown.

No additional error from level 3 (Fig. 6.1) is introduced in level 4 for the calculation of CDIST. The calculation of CDIST simply flags cells according to the distance away from hard over soft contacts. Error in calculating dip and orientation from the structure surface are similar to topographic slope and aspect calculations in that they are averaged 60 m vector calculations and the location and amount of error is unknown. The structure contour error is thought to be less than topographic error because of the relatively uniform nature of stratigraphic layers compared to the fractal nature of topography.

Level 5 (Fig. 6.1.) represents the error of the combined topographic and structure data sets in calculating STYPE. In calculating slope type, the error in both the topographic aspect and the structure orientation are combined. Error in this calculation would cause some slope type misclassification. Some cataclinal slopes may be misclassified as plagioclinal slopes and plagioclinal slopes may be misclassified as cataclinal slopes. In classifying cataclinal slopes into underdip and overdip the error of topographic SLOPE and structure dip are included in STYPE. Because SLOPE is an average over 60 m it will have a lower gradient than actual slopes within the average. The comparison of structure dip with averaged SLOPE will misclassify some slopes as cataclinal overdip that should be classified as cataclinal underdip according to true slope. With this topographic averaging bias overdip slopes, which are critical to prediction of slope instability, will tend to be misclassified as underdip slopes but it is unlikely that underdip slopes will be misclassified as overdip slopes.

The statistical analysis which is used for prediction is based on the use of SLOPE, MTYPE, CDIST and STYPE with the cumulative amount of error (level 6; Fig. 6.1.) incorporated at each level for each factor. The analysis effectively discriminates between FAIL and NFAIL (with landslide locations at ±250 m resolution) from the values of SLOPE (filtered and averaged 60 m gradient), MTYPE (homogenous classification of majority material type in 30 m cell with ±60 m resolution), CDIST (averaged to 30 m cells with ±60 m resolution) and STYPE (combined error of topographic aspect and structure orientation with a combined error of topographic SLOPE and structure dip and at least ±320 m resolution). STYPE is not significant, but SLOPE, MTYPE and CDIST are used in the final discriminant analysis.

The total amount of error in the analysis is not directly determinable, however, the total error is empirically suggested to be ±250 m, as shown on the top of Figure 6.1. There are two lines of evidence which support 250 m of uncertainty. First, the resolution to which FAIL is mapped is ±250m. Second, in the comparison of FAIL and CDIST, 65% of FAIL are within 250 m of h/s contact. Mechanically the correlation of h/s contacts and instability is logical in that an underlying weaker unit will erode faster than an overlying resistant unit, creating slope failure potential. There should not be a decrease in slope failure hazard with increasing distance from a h/s contact, therefore the apparent decrease to ~250 m probably represents accumulated error.

Recommended Use of This Study

With the described types of error and ±250 m of empirically determined location error in the analysis how can the prediction of slope instability be used? It is clear the resolution and error of this study will not allow site evaluation at lot-size scales. For a site evaluation an accurate gradient is necessary, rather than a 60 m average slope from a filtered DEM. Detailed topographic are required because even a small cliff may not be visible as such in a calculated slope. Detailed material characteristics would also be desirable, rather than a classified material type averaged over 30m. It would also be wise to closely evaluate faults, fractures, bedding planes and all other discontinuities rather than just the general structure orientation.

Even though this study does not give site specific information it does show that slope instability hazard potential does exist in some areas of Yellowstone County where failure has not been mapped. Awareness of a hazard is the first step toward avoidance of such a hazard. This study points out that SLOPE and CDIST are important factors in a regional slope instability analysis. Results of this study summarize general areas of high instability and low instability for regional evaluation. For very low probabilities of FAIL (< 0.30) the model correctly predicts 88% of existing combinations used in the discriminate as NFAIL (combinations listed in Appendix by increasing probability of failure). For very high probabilities of FAIL (> 0.96) the model correctly predicts 100% of existing factor combinations as FAIL (note tails of NFAIL and FAIL in Fig. 5.2). This indicates a high accuracy for correctly predicting high and low probabilities of FAIL. Where probabilities of failure are high or moderate additional site specific data is very important before concluding development should proceed.

Stability studies are often the basis of zoning regulations for building and development. At the time of this study no such zoning regulations regarding slope stability are planned. If this study were to be used as a basis for zoning regulation it would be best used in the following manner. First the statistical probability of hazard critical for zoning must be identified. If the identified level of hazard necessary for zoning was determined as a probability of FAIL ≥0.50 then only areas with ≥0.50 probability of failure would be in a special zoning area. Areas in the special zoning area could be required to have a site evaluation and meet determined standards for safe construction and development in areas of potential slope failure.

Contributions of This Study

This study directly provides a planning tool for Yellowstone County, Montana, and demonstrates a workable method for regional evaluation of slope instability hazard which can be readily used in other areas. GIS, used as the spatial analytical tool in this study, is becoming more available in local governments. SLOPE, the strongest predictor in this study, is derived from US Geological Survey DEMs, available for many areas. A new method is presented for filtering out noise inherent in 30 m DEMs that gives smooth slope calculation with less error than standard filters. MTYPE and CDIST are both derived from published geologic maps at regional scales. Geologic maps may be available for other locations but the scale and areal extent will vary.

This study also points to the importance of h/s contacts in predicting rock slope instability in Yellowstone County, Montana, and hints at the importance of h/s contacts to rock slope instability elsewhere. Material type was dominantly used in other studies but was not critical here.

Even though the incorporation of bedding discontinuities is unsuccessful in this study, some issues are highlighted that need to be evaluated in considering bedding discontinuities and slope type in slope instability hazard evaluation. Structure contours are introduced herein for generalizing bedding discontinuities. With a better-than-30 m topographic resolution, an STYPE calculation may be significant for stability analysis for some areas. Calculated slope with an effective average over 60 m may have reduced the effectiveness of this variable as a predictor.

Suggested Further Study

The CDIST factor is significant for predicting slope instability. This factor is more important than MTYPE in this study. Further study is needed to determine the significance h/s contacts are in other areas. Further study could evaluate the mechanics of h/s contact failures and determine the relationship between the h/s contact environment and failure.

STYPE was not a predictor in this study but is in others. Further work is needed to evaluate bedding discontinuities in a regional analysis. A method needs to be developed for accurately representing discontinuities in GIS at a regional analysis. Failing this, site specific collection methods may need to be developed. Slope type could be measured at FAIL and NFAIL locations but then a similar measurement would be needed in all areas to predict probability of FAIL.

The limiting factor of resolution in this study is the 30 m DEM. Further study is needed to better understand the meaning of slope in a 30 m cell. Is there a way to determine if and how 30 m slopes differ from one region to another? If there was a way to calculate the likely maximum and minimum slope within a 30 m slope, would it be of use in determining the probability of failure in a 30 m cell?

The largest source data uncertainty was the location of the landslides. Improving the locations of mapped landslides from the 250 m to a 30 m resolution could improve the statistical analysis. Error from misclassification of FAIL locations due to the map scale resolution could be eliminated.

Further analysis of data used in this study may produce more confident results. An analysis that may be useful is calculation of the worst-case stability for 9X9 windows of the 30 m cells. For each mapped landslide location the worst-case probability of failure would be assigned. Analysis in this manner may solve the problem of the resolution of mapped landslides and the overall locational inaccuracy.

REFERENCES CITED

Alexander, D., and Formichi, R., 1993, Tectonic causes of landslides: Earth Surface Processes and Landforms, v. 18, p. 311-338.

Bernknoff, R. L., Campbell, R. H., Brookshire, D. S., and Shapiro, C. D., 1988, Probalistic approach to landslide hazard mapping in Cincinnati, Ohio, with applications for economic evaluation: Bulletin of the Association of Engineering Geologists, v. 25, p. 39-56.

Bonham-Carter, G. F., 1994, Geographic Information Systems for Geoscientists, Modeling with GIS: Tarrytown, New York, Elsevier Science Inc., 398 p.

Briggs, R. P., Pomeroy, J. S., and Davies, W. E., 1975, Landsliding in Allegheny County, Pennsylvania: U.S. Geological Survey Circular 728, 18 p.

Carrara, A., 1983, Multivariate models for landslide hazard evaluation: Mathematical Geology, v. 15, p. 403-426.

Carrara, A., Caradinali, M., Detti, R., Guzzetti, F., Pasqui, V., and Reichenbach, 1991, GIS techniques and statistical models in evaluating landslide hazard: Earth Surface Processes and Landforms, v. 16, p. 427-445.

Churchill, R. R., 1982, Aspect-induced differences in hillslope processes: Earth Surface Processes and Landforms, v. 7, p. 171-182.

Cruden, D. M., 1985, Rock slope movements in the Canadian Cordillera: Canadian Geotechnical Journal, v. 22, p. 528-540.

Cruden, D. M., 1988, Thresholds for catastrophic instabilities in sedimentary rock slopes, some examples from the Canadian Rockies: Zeitschrift fur Geomorphologie, Supplement 67, p. 67-76.

Cruden, D. M., 1989, Limits to common toppling: Canadian Geotechnical Journal, v. 26, p. 737-742.

Cruden, D. M., and Eaton, T.M., 1987, Reconnaissance of rockslide hazard in Kananaskis country, Alberta, Canada: Canadian Geotechnical Journal, v. 24, p. 414-429.

Cooke, R. U., and Doornkamp, J. C., 1990, Geomorphology and environmental management, Second Edition: Oxford University Press, New York, p. 106-129.

Duncan, S. H., Ward, J. W., and Anderson, R. J., 1987, A method for assessing landslide potential as an aid in forest road placement: Northwest Science, v. 61, p.152-159.

Eklundh, L., and Martensson, U., 1995, Rapid generation of Digital Elevation Models from topographic maps: International Journal of Geographic Information Systems, v. 9, p. 329-340.

Elassal, A. A., and Caruso, V. M., 1984, Digital elevation models: U.S. Geologic Survey Circular 895-B, 40 p.

ESRI, 1991, Cell-based Modeling with Grid, ARC/INFO Users Guide: Environmental Research Systems Institute, Redlands, California, 303 p.

Gao, J., and Lo, C. P., 1991, GIS Modeling of the influence of topography and morphology on landslide occurrence in Nelson County, Virginia: GIS/LIS 1991 Proceedings, American Society for Photogrammetry, v. 2, p. 954-963.

Gosling, A. W., and Pashley, E. F., Jr., 1973, Water resources of the Yellowstone River valley, Billings to Park City: U.S. Geological Survey, Hydrologic Investigations, Atlas HA-454, Sheet 1, Scale 1:48,000.

Gupta, R. P., and Joshi, B. C., 1990, Landslide hazard zoning using the GIS approach - a case study from the Ramganga Catchment, Himalayas: Engineering Geology, v. 28, p. 119-131.

Hancock, E. T., 1919, Geology and oil and gas prospects of the Lake Basin Field, Montana: U.S. Geological Survey, Bulletin 691, Plate 16, Scale 1:125,000.

Hancock, E. T., 1920, Geology and oil and gas prospects of the Huntly Field, Montana: U.S. Geological Survey, Bulletin 711, Plate 14, Scale 1:125,000.

Heine III, G. W., 1986, A controlled study of some two-dimensional interpolation methods: COGS Computer Contributions, v. 2, p. 60-72.

Jibson, R. W., and Keefer, D. K., 1989, Statistical analysis of factors affecting landslide distribution in the New Madrid seismic zone, Tennessee and Kentucky: Engineering Geology, v. 27, p. 509-542.

Knappen, R. S., and Moulton, G. F., 1930, Geology of parts of Carbon, Yellowstone, Big Horn, and Stillwater Counties, Montana: U.S. Geological Survey, Bulletin 822, Plate 1, Scale 1:125,000.

Lessing, P., Messina, C. P., and Fonner, R. F., 1983, Landslide risk assessment: Environmental Geology, v. 5, p. 93-99.

National Research Council, 1985, Reducing losses from landsliding in the United States: Committee on ground failure hazards commission on engineering and technical systems, National Academy Press, Washington, D.C., 32 p.

Mills, R. L., 1987, Landslide hazard, Montana *in*: Hazard and Vulnerability Analysis: Department of Military Affairs, Helena, Montana, 161 p.

Selby, M. A., 1980, A rock mass strength classification for geomorphic purposes with tests from Antarctica and New Zealand: Zeitschrift fur Geomorphologie, v. 24, p. 31-51.

Soil Conservation Service, 1972, Soil survey of Yellowstone County, Montana, 145 p.

Tabachnick, B.G., and Fidell, L.S., 1989, Using Multivariate Statistics, Second Edition, Harper Collins Publishers, Inc., New York, NY, 746 p.

Terzaghi, K., 1962, Stability of steep slopes on hard unweathered rock: Geotechnique, v. 12, p. 251-270.

Thompson, M. M., 1979, Maps for America: U.S. Geological Survey, 245 p.

Thom, W. T., Jr., Hall, G. M., Wegemann, C. H., and Moulton, G. F., 1935, Geology of Big Horn County and the Crow Indian Reservation, Montana, with special reference to the water, coal, oil, and gas resources: U.S. Geological Survey, Bulletin 856, Plate 1, Scale 1:187,000.

Wadge, G., 1988, The Potential of GIS modelling of gravity flows and hillslope instabilities: International Journal of Geographical Information Systems, v. 2, p. 143-152.

Wieczorek, G. F., Wilson, R. F., and Harp, E. L., 1985, Map showing slope stability during earthquakes in San Mateo County, California: U.S. Geological Survey Miscellaneous Field Studies Map I 1257-E, Scale 1:500,000.

Wilde, E. M., Colton, R. B., Bartholomew, M. A., Daniel, E. E., Dresser, H. W., Stickney, M. C., Brabb, E. E., Derkey, E. S., and Vokt, E. S., unpublished, Preliminary map of landslides in Montana, Scale 1:62,500.

Yellowstone County Department of Planning, 1990, Yellowstone County Comprehensive Plan, 410 North Broadway, Billings, Montana

APPENDIX

Data list of all existing factor combinations of the model input data, ranked in order of increasing probability of failure.

Group	* Correct Group Prediction	SLOPE	MTYPE	CDIST	Frequency	Probability of Failure
NFAIL	*	2	3	4	22	0.122
FAIL		2	3	4	1	0.122
NFAIL	*	2	2	4	44	0.159
FAIL		2	2	4	2	0.159
NFAIL	*	4	3	4	7	0.180
NFAIL	*	2	3	3	2	0.199
NFAIL	*	2	1	4	146	0.205
FAIL		2	1	4	20	0.205
NFAIL	*	4	2	4	12	0.230
NFAIL	*	2	2	3	6	0.253
NFAIL	*	6	3	4	5	0.258
NFAIL	*	4	3	3	1	0.283
FAIL		4	3	3	1	0.283
NFAIL	*	4	1	4	47	0.290
FAIL		4	1	4	16	0.290
NFAIL	*	2	3	2	1	0.309
NFAIL	*	2	1	3	11	0.316
FAIL		2	1	3	3	0.316
NFAIL	*	6	2	4	8	0.322
NFAIL	*	4	2	3	2	0.350
FAIL		4	2	3	1	0.350
NFAIL	*	8	3	4	3	0.355
FAIL		8	3	4	1	0.355
NFAIL	*	2	2	2	3	0.379
FAIL		2	2	2	2	0.379
NFAIL	*	6	3	3	1	0.385
NFAIL	*	6	1	4	33	0.393
FAIL		6	1	4	10	0.393
NFAIL	*	4	3	2	1	0.415
NFAIL	*	4	1	3	6	0.423
FAIL		4	1	3	4	0.423
NFAIL	*	8	2	4	3	0.429
NFAIL	*	2	3	1	2	0.445
NFAIL	*	2	1	2	6	0.454
FAIL		2	1	2	2	0.454
NFAIL	*	6	2	3	1	0.460
NFAIL	*	10	3	4	1	0.466
FAIL		10	3	4	1	0.466
NFAIL	*	4	2	2	1	0.491
FAIL		4	2	2	1	0.491
FAIL		8	3	3	1	0.497
NFAIL		8	1	4	18	0.506
FAIL	*	8	1	4	9	0.506
NFAIL		2	2	1	3	0.523
FAIL	*	2	2	1	3	0.523
FAIL		6	1	3	4	0.537
FAIL	*	6	1	3	2	0.537
NFAIL		10	2	4	1	0.543
NFAIL		4	3	1	1	0.560
NFAIL		4	1	2	3	0.568
FAIL	*	4	1	2	2	0.568
NFAIL		12	3	4	1	0.580
NFAIL		2	1	1	7	0.599
FAIL	*	2	1	1	2	0.599

Group	* Correct Group Prediction	SLOPE	MTYPE	CDIST	Frequency	Probability of Failure
NFAIL		6	2	2	1	0.605
FAIL	*	6	2	2	1	0.605
NFAIL		10	1	4	10	0.619
FAIL	*	10	1	4	8	0.619
NFAIL		4	2	1	1	0.634
FAIL	*	4	2	1	2	0.634
NFAIL		8	1	3	2	0.648
FAIL	*	8	1	3	2	0.648
NFAIL		12	2	4	1	0.653
NFAIL		6	3	1	1	0.668
NFAIL		6	1	2	2	0.676
FAIL	*	6	1	2	1	0.676
FAIL	*	10	2	3	1	0.681
NFAIL		14	3	4	1	0.686
FAIL	*	14	3	4	1	0.686
NFAIL		4	1	1	4	0.703
FAIL	*	4	1	1	2	0.703
FAIL	*	8	2	2	5	0.708
FAIL	*	12	3	3	1	0.713
NFAIL		12	1	4	7	0.720
FAIL	*	12	1	4	7	0.720
NFAIL		6	2	1	1	0.733
NFAIL		10	1	3	2	0.744
FAIL	*	14	2	4	1	0.749
NFAIL		8	1	2	1	0.768
FAIL	*	8	1	2	1	0.768
NFAIL		6	1	1	3	0.789
FAIL	*	6	1	1	4	0.789
FAIL	*	10	2	2	1	0.793
NFAIL		14	1	4	5	0.803
FAIL	*	24	1	4	1	0.976
NFAIL		14	1	3	1	0.880
FAIL	*	14	1	3	1	0.880
FAIL	*	12	1	3	2	0.822
NFAIL		10	1	2	1	0.839
NFAIL		8	1	1	2	0.856
FAIL	*	8	1	1	1	0.856
NFAIL		16	1	4	3	0.866
FAIL	*	16	1	4	1	0.866

Group	* Correct Group Prediction	SLOPE	MTYPE	CDIST	Frequency	Probability of Failure
NFAIL		12	1	2	1	0.892
FAIL	*	12	1	2	3	0.892
NFAIL		10	1	1	1	0.904
FAIL	*	10	1	1	1	0.904
FAIL	*	14	3	2	1	0.876
NFAIL		18	1	4	2	0.911
FAIL	*	18	1	4	2	0.911
FAIL	*	16	1	3	3	0.920
FAIL	*	14	1	2	2	0.929
NFAIL		12	1	1	1	0.937
FAIL	*	12	1	1	1	0.937
FAIL	*	16	2	2	1	0.938
NFAIL		20	1	4	1	0.942
FAIL	*	20	1	4	3	0.942
NFAIL		14	1	1	1	0.959
FAIL	*	14	1	1	1	0.959
FAIL	*	22	1	4	2	0.962
FAIL	*	16	2	1	2	0.965
FAIL	*	20	1	3	1	0.967
FAIL	*	18	1	2	1	0.971
FAIL	*	26	3	4	1	0.972
FAIL	*	20	1	2	1	0.981
FAIL	*	18	1	1	2	0.983
FAIL	*	24	1	3	1	0.986
FAIL	*	22	1	2	1	0.988
FAIL	*	20	1	1	2	0.989
FAIL	*	26	1	3	1	0.991
FAIL	*	24	1	2	1	0.992
FAIL	*	22	1	1	1	0.993
FAIL	*	24	1	1	1	0.996
FAIL	*	28	2	1	1	0.998
FAIL	*	28	1	1	1	0.998
FAIL	*	14	1	4	5	0.803
FAIL	*	8	2	1	2	0.813
NFAIL		12	1	3	1	0.822
FAIL	*	10	2	1	1	0.873
NFAIL		16	1	1	1	0.974
FAIL	*	24	3	3	1	0.975